# BRAIN SYSTEM MECHANISMS UNDERLYING DEVELOPMENTAL CHANGES IN WORKING MEMORY PERFORMANCE DURING ADOLESCENCE

by

**David Florentino Montez**

B.S., California State University East Bay, 2008

Submitted to the Graduate Faculty of

the School of Medicine in partial fulfillment

of the requirements for the degree of

Doctor of Philosophy

University of Pittsburgh

2016

UNIVERSITY OF PITTSBURGH

School of Medicine

This dissertation was presented

by

David Florentino Montez

It was defended on

November 11, 2016

and approved by

Beatriz Luna, Ph.D., Department of Psychiatry, University of Pittsburgh

Julie A. Fiez, Ph.D., Department of Psychology, University of Pittsburgh

Carl R. Olson, Ph.D., Center for Neuroscience, University of Pittsburgh

Timothy D. Verstynen, Ph.D., Department of Psychology, Carnegie Mellon University

Tobias Teichert, Ph.D., Department of Psychiatry, University of Pittsburgh

Michael Hallquist, Ph.D., Department of Psychology, Penn State University

Dissertation Advisor: Beatriz Luna, Ph.D., Department of Psychiatry, University of Pittsburgh

**BRAIN SYSTEM MECHANISMS UNDERLYING DEVELOPMENTAL CHANGES IN WORKING MEMORY PEFORMANCE DURING ADOLESCENCE**

David F. Montez, Ph.D.

University of Pittsburgh, 2016

Working memory is a critical component of executive function that continues to develop during adolescence. In addition to developmental improvements in mean performance, there are significant decreases in behavioral variability. The neural underpinnings of developmental changes in behavioral variability are poorly understood although they would provide important insight into the nature of improvements in working memory. This dissertation takes a multilevel approach, applying whole-brain fMRI analyses and computational modeling to a longitudinal data set acquired from a cohort of 8-30 year olds as they performed a memory guided saccade task.

First, we delineate behavioral changes in trial-to-trial in performance variability and explore these changes within a drift diffusion framework. We find that a trial-to-trial variations in gain and response thresholds accounts for features of behavioral instability. Second, we establish that trial-to-trial behavioral variability is associated with fluctuations in the expression of whole brain patterns of task-related BOLD signal, or brain state variability, which is a predicted consequence of widespread gain modulation. We find that individual trajectories of developmentally stabilizing behavior are predicted by changes in brain state variability. Third, in order to explore reports of a relationship between the complexity of neural activity and behavioral stability, we characterize developmental increases in BOLD complexity in a task context and assess their

relationship to developmental changes in behavior. Collectively, our findings provide novel evidence that the age-related stabilization of behavioral performance is driven by the stabilization of widespread gain signals across development.

## TABLE OF CONTENTS

## LIST OF EQUATIONS

## LIST OF FIGURES

# 1.0 INTRODUCTION

## 1.1 WORKING MEMORY AND COGNITIVE CONTROL

A core aspect of cognition and cognitive control is working memory, the ability to maintain information online in the service of goal-directed behavior [1]. The basic processes that support working memory are available as early as infancy [2] but continue to develop throughout adolescence [3], [4]. Working memory exhibits a prolonged time course of maturation relative to other cognitive processes [5], [6]. For instance, performance is disproportionately impaired during early adolescence, when difficulty is increased, such as when multiple items need to be remembered, or remembered information must be manipulated [7], [8]. The ability to direct saccades during cognitively demanding tasks is online by age 15, when reaction time and accuracy reaches mature levels. However, the precision of saccades made to a remembered location continues to improve until late in the second decade of life, even after reaction times have stabilized [5]. That this effect is still present regardless of the delay length suggests 1) that development of processes other than those involved in maintenance, e.g., encoding and retrieval, may contribute to developmental improvements in working memory; and 2) the fidelity of motor responses based on

working memory representations may be an additional site of continued developmental improvement.

## 1.2 BEHAVIORAL VARIABILITY AND DEVELOPMENT

Even under ideal conditions, subjects are rarely able to perform a behavioral response multiple times in exactly the same way; reaction times shift, accuracy varies, and occasionally there is a failure to perform altogether. This kind of instability in responding is known as behavioral variability or, occasionally, intra-individual variability.

Behavioral variability has long been known to be a sensitive measure for a variety of cognitive and psychiatric disorders including attention-deficit hyperactivity disorder (ADHD) [9]; schizophrenia, depression and borderline personality disorder [10]; traumatic brain injury, dementia, and —more generally— with overall cognitive decline [11]). Thus, behavioral variability may also provide insight into the normative development of processes like working memory that support cognition. Recently this idea has been explored in an emerging literature.

Roughly, theses efforts can be broken up into two groups: those that attempt to link developmental changes in behavioral variability to changes in brain structure, and those that link it to changes in neural activity. Reduced white matter integrity is associated with increased behavioral variability in adults performing the Eriksen flanker task [12]. In combination with longitudinal analyses of normative adolescent populations, which reveal that reaction time across flanker task trials stabilizes in

parallel with developmentally increasing tract integrity [13], a story begins to emerge in which behavioral variability decreases as brain structure matures. It is unclear however, what mechanisms that would cause greater white matter integrity to result in more consistent behavior.

The story becomes complicated when considered in light of developmental changes in neural variability rather than structural integrity. A highly replicable finding is that temporal patterns of neural activity become increasingly complicated with age. Magnetoencephalographic (MEG) measures of neural signal complexity, such as dimensionality and mutli-scale entropy, increase across adolescence in tandem with stabilizing behavioral variability [14]-[16]. Certain aspects of developmental fMRI data are consistent with these findings. Within network resting state connectivity decreases during adolescence as one might predict if neural activity were truly becoming more complex across the brain [17].

It is not clear however what role structural maturation plays in the changes in neural activity. One possibility is that as white matter integrity matures, the neural signal-to-noise ratio improves, thereby providing a mechanism for stabilizing behavior [12]. However, squaring this idea with the observations that neural activity is actually increasing in complexity (and is therefore, in a sense, becoming more variable) requires further exploration. One current hypothesis that attempts synthesis states that as white matter integrity increases, greater potential integration between brain regions is allowed, which fosters the dynamic construction of a greater number of states of activity and facilitates transitions between them [14], [15]. It has also been proposed that the additional complexity represent beneficial noise that improves cognitive processes [14].

# 2.0 DEVELOPMENTAL CHANGES IN SPATIAL WORKING MEMORY PERFORMANCE

## 2.1 BACKGROUND

The memory-guided saccade task was initially developed to isolate the sensory and motor components of neural activity driving the production of saccadic eye-movements, [18]. In the earliest experiments using this task, a monkey, trained to maintain fixation on a central point, was briefly presented with a peripheral stimulus. After a short delay period, the animal performed a saccade, generated in the absence of any relevant visual sensory information, to the remembered location of the target. These early electrophysiological experiments, performed in the substantia nigra, found neurons that could be roughly classified based on whether they responded (with reduced firing) to the stimulus, the saccadic eye-movement itself, or (surprisingly) during the delay interval between the target presentation and saccadic response. The researchers described this last “memory-contingent” category of neurons as behaving as though they “maintained information on the approximate location of the target cue to enable a delayed saccade to the location of the target.” Later, this task was applied by others who found neurons exhibiting saccade-related delay period activity in prefrontal cortex (PFC) [19]. In combination with behavioral deficits observed in patients with PFC lesions as they

performed other delayed response tasks, these findings contributed substantially to the perception that PFC was a key site for the temporary storage of working memory information [20]. More recently, there is increasing evidence that the capability to sustain information on line is available throughout much of the brain, and that delay period activity in PFC is more closely related to representing abstract features, rules, and demands of particular tasks [21].

Consistent with this, single unit studies in non-human primates have revealed the presence of memory contingent, or preparatory, responses in such widespread regions as the intermediate layers of the superior colliculus [22], parietal cortex [23], and the frontal eye field [24]. fMRI studies of adult humans show similar patterns of widely distributed circuitry [25]. Moreover, whole-brain multivariate pattern analyses have demonstrated that stimulus specific information can decoded from delay-period activity within sensory cortex [26], [27], suggesting that working memory activity is sustained by processes that are similar to sensory recruitment.

Developmental researchers, charting trajectories of oculomotor performance throughout childhood and adolescence, found that the peak velocity of saccades reaches mature levels around the 4$^{th}$—6$^{th}$ years of age [28], [29]. Additionally, the higher order psychophysical relationship between saccadic amplitude and peak velocity —the so-called main sequence— is also present and adult-like by the same time [28], [30]. However, measures of reaction time (thought to index the speed of sensory and cognitive processing) and accuracy exhibit monotonic improvements that continue until roughly 15 years of age [5], [28], [31]. The accuracy of secondary corrective memory-guided saccades continues to improve until very near the 20$^{th}$ year however [5].

Together, these findings suggest while the oculomotor system matures very early, cognitive processes that engage the eye-movement machinery still continue to develop and refine. The mechanisms that allow eye-movements to be driven by working memory representations, in particular, appear to exhibit the most prolonged time course of maturation.

Determining what neural changes underlie developmental improvement in memory guided saccade performance has proven to be a challenge. A particularly vexing confound arises from the structure of the memory-guided saccade task itself: the initial presentation of a target stimulus at the start of each trial occurs as the subject is fixating a central stimulus, and trials are considered incorrect if a subject breaks fixation to look at the target. Because younger subjects often have great difficulty not looking at targets as they are presented [32], a conceptual concern is that younger subjects may be exerting much greater effort suppressing an exogenously driven orienting response. Therefore, age-related difference in effort could result in differences in neural or BOLD responses that do not reflect true changes in the circuitry supporting task performance, but instead reflect the differential engagement of processes related to response inhibition. For these experiments, we employ a version the memory-guided saccade task designed to reduce demands of response inhibition by eliminating the need to suppress the initial orienting eye-movement.

In addition, because spatial working memory is not a single monolithic process, developmental changes in behavioral performance may result from independent refinements of its constituent processes. Working memory can be conceived as consisting of three component processes: encoding, maintenance, and retrieval.

Encoding is the process of instantiating a context-appropriated persistent neural state for the purpose of guiding future goal-directed behavior. Maintenance refers to the processes that sustain the encoded neural information. Retrieval is the processes through which a particular working memory representation is selected and mapped onto an appropriate motor response. In this construction, both encoding and maintenance could theoretically affect the fidelity of information maintained in working memory and the facility with which it can be drawn upon in the future. Developmental changes in behavioral performance during the memory-guided saccade task a can potentially be attributed maturation affecting either or both of these two processes. To explore this possibility, we modified the memory-guided saccade task to allow measurements of the effects of encoding and maintenance duration across development.

With the preceding in background in mind, we set out to address the following two questions for our first set of analyses.

**I.** Chart longitudinal developmental changes in behavioral performance, focusing particularly on behavioral variability, using a memory-guided saccade that controls for age-related confounds related to response inhibition.

**II.** To explore the mechanisms underlying the seemingly prolonged maturation of spatial working memory performance and their relationship to different aspects of behavioral variability.

## 2.2 TASK DESIGN

In our version of the memory-guided saccade task, performed in an fMRI scanner, subjects first fixated a central yellow cross which, after a pseudo-randomly selected

inter-trial interval (ITI) drawn from a 3-12 second range, disappeared and was replaced by a small circular yellow target positioned unpredictably at one of six locations (±3º, 6º or 9º of visual angle) along the horizontal visual meridian (Figure 1**a**). The stimulus remained visible during a presentation interval of either 1.5 or 3 seconds. The subjects were instructed to make an eye-movement to and fixate upon the stimulus while it was present. At the end of the presentation interval, the target stimulus disappeared and the central fixation-cross reappeared, marking the beginning of the delay interval. Subjects reoriented their gaze to the fixation cross while maintaining the previously executed location for either 1.5 or 9 seconds. The disappearance of the central fixation cross signaled the end of the delay interval, and subjects were instructed to quickly and accurately perform an eye movement to the remembered location of the target stimulus in the absence of any sensory guidance. The two durations of delay and presentation intervals results in four primary task conditions. Stimuli were presented using E-Prime (Psychology Software Tools, Inc., Pittsburgh, PA), projected onto a flat screen positioned behind the magnet. Participants viewed the screen using a mirror mounted on the RF head coil. Behavioral performance was measured under four conditions corresponding to each combination of short and long presentation and delay intervals. Subjects performed 15 trials from each of the four primary task conditions, for 60 total trials, which were divided evenly across 3 task blocks.

The distinguishing feature of our variant of the memory-guided saccade task is that subjects were instructed to make a visually guided encoding saccade to the target stimulus, rather than maintain fixation during its presentation. Allowing subjects to perform the initial visually guided saccade was done to minimize age-related sources of

behavioral differences that are related to response inhibition rather than working memory performance. This design also allowed us to isolate the concurrent visuomotor/encoding and retrieval responses that comprise the BOLD signal evoked by a memory-guided saccade, a fact that we exploit during our analysis the fMRI data (see Chapter 2). We monitored the subject's gaze in the scanner with an infrared camera and eye-tracking system.

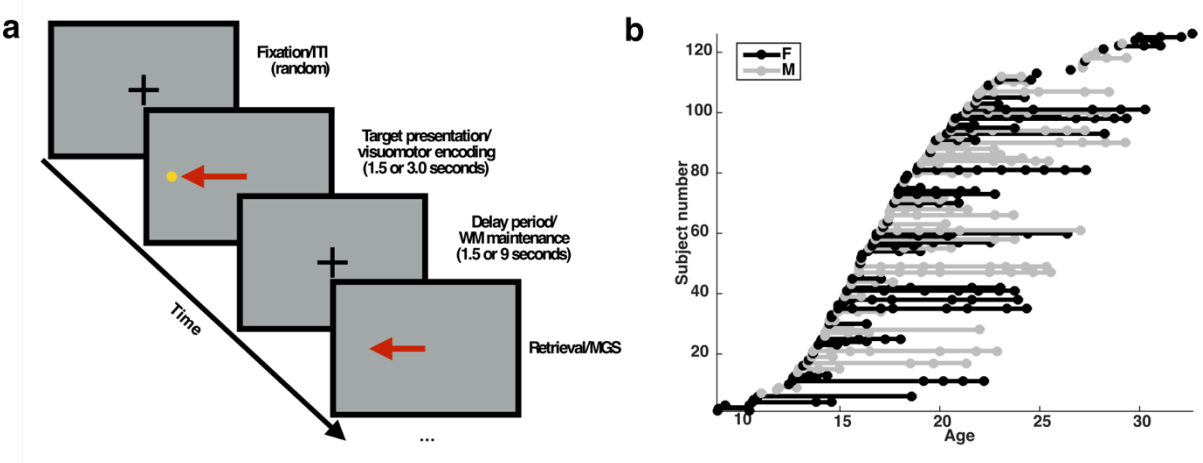


**Figure 1. Task design and subject distribution**

**a) A schematic depiction of the variant of the memory-guided saccade task employ in our study. b) The distribution of subjects included in our analyses. Each entry on the y-axis represents a unique subject. A single visit is indicated by a dot whose x-coordinate corresponds to the age of the subject at that visit. A solid line connects repeated sessions**

## 2.3 SUBJECTS

We tested 126 healthy subjects (60 female) between the ages of 8 and 33 years. Subjects were initially recruited between the ages of 8.9 and 29.8 years and were scanned approximately annually for 1-10 years (Figure 1**b**). Participants and/or their legal guardians provided informed consent before participating in this study. Experimental procedures for this study complied with the Code of Ethics of the World Medical Association (1964; Declaration of Helsinki) and the Institutional Review Board at the University of Pittsburgh. Subjects were paid for their participation in the study.

## 2.4 METHODS

We extracted two measurements from each trial: 1) reaction time, the interval between the extinction of the fixation stimulus at the end of the delay interval and the initiation of the memory-guided saccade and 2) saccadic error, the signed visual angle separating the horizontal location of the target and the end point of the memory-guided saccade. For the four task conditions during a session, we computed mean and standard deviation of reaction time, as well as summary measures to characterize accuracy and precision. We defined saccade accuracy as absolute value of average saccadic error for a given target, and saccade precision as the standard deviation of saccadic error for each target. Behavioral results are depicted in Figure 2a-d.

Most analyses were performed using the linear mixed-effects, or multi-level, statistical framework, which has been formalized to deal with differing numbers of repeated measurements. This feature makes that approach particularly well suited to the analysis of longitudinal developmental data, where unpredictable attrition within the returning subject pool makes it very difficult to perform the same number of measurements on every subject.

We modeled developmental changes in behavioral performance using the following formula:

Where:

**Equation 1. Behavioral regression model**

$$\boldsymbol{Behavior} \sim \mathbf{1} + \boldsymbol{Age}_{\boldsymbol{first}}^{\mathbf{-1}} + \boldsymbol{Age}_{\boldsymbol{relative}}^{\mathbf{-1}} + \left(\boldsymbol{PI} * \boldsymbol{Age}_{\boldsymbol{first}}^{\mathbf{-1}}\right) + \left(\boldsymbol{PI} * \boldsymbol{Age}_{\boldsymbol{relative}}^{\mathbf{-1}}\right) + \left(\boldsymbol{DI} * \boldsymbol{Age}_{\boldsymbol{first}}^{\mathbf{-1}}\right) + \left(\boldsymbol{DI} * \boldsymbol{Age}_{\boldsymbol{relative}}^{\mathbf{-1}}\right) + \left(\mathbf{1} + \boldsymbol{Age}_{\boldsymbol{relative}}^{\mathbf{-1}} | \boldsymbol{ID}\right)$$

**I.** Behavior is the log transformation of a particular behavioral measure, e.g., mean or standard deviation of reaction time.

**II.** $PI$ and $DI$ are dummy coded zero-mean values where -1 and 1 were used to represent short and long presentation and delay intervals respectively.

**III.** $Age_{first}^{-1}$ is the inverse of a subject's age at their first visit.

**IV.** $Age_{relative}^{-1} = Age^{-1} - Age_{first}^{-1}$

**V.** $ID$ is a unique categorical variable assigned to each subject.

**VI.** $(1 + Age_{relative}^{-1}|ID)$ indicates that the linear mixed-effects model contained a random offset and slope for each subject.

It is worth emphasizing that the $x^{-1}$ form of the $Age_{first}^{-1}$ and $Age_{relative}^{-1}$ terms implies that the magnitude of a variable's change, for a given time interval, decreases

with age. This allows us to model the expectation that developmental changes in behavioral performance should decrease in magnitude across age.

## 2.5 RESULTS

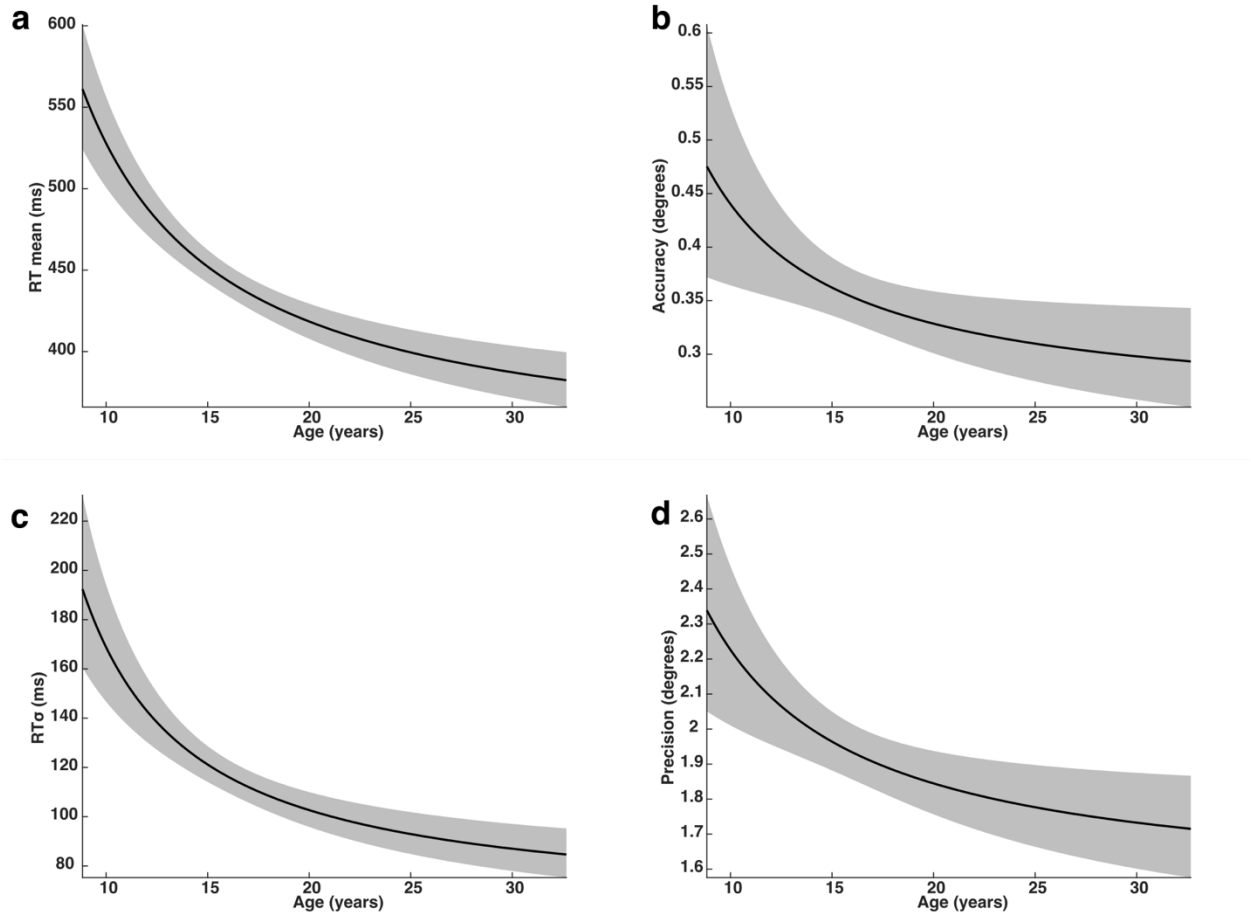


**Figure 2. Change in behavioral performance across development**

**Depicts the changes across age in a) mean reaction time; b) accuracy (average saccadic error); c) reaction time variability (standard deviation); and d) precision of memory-guided saccades (standard deviation of saccadic error). Each black curve depicts the**

**best fitting group-level 1/age trajectory. The gray envelope represents the 95% confidence bounds.**

### 2.5.1 Main effects of task on behavioral performance

#### *Average reaction time*

Changes in the duration of the presentation interval did not affect subject's reaction times (t(1334)=0.62, p=0.52). As expected reaction times were much faster on trials with longer delay intervals (t(1334)=-5.27, p=1.55e-7). We observed no significant interaction effect between the duration of the presentation and delay intervals (t(1334)=-1.04, p=0.3).

#### *Accuracy*

We observed no significant effects of presentation (t(1334)=-0.45, p=0.65), delay interval (t(1334)=-0.07, p=0.94), or their interaction (t(1334)=1.48, p=0.14 on accuracy.

#### *Reaction time variability*

Similarly, the presentation interval did not appear to influence reaction time variability (t(1334)=-0.18, p=0.98). Longer delay intervals were associated with significantly reduced reaction time variability (t(1334)=-3.77, p=1.6e-4). There was no significant interaction (t(1334)=1.5, p=0.14).

#### *Precision*

The precision of memory-guided saccades were mostly unaffected by altering the presentation interval (t(1334)=-1.57, p=0.12), while longer delay intervals were associated with reduced precision (t(1334)=3.11, p=1.8e-3). The interaction between presentation and delay intervals was insignificant (t(1334)=-1.01, p=0.31).

### 2.5.2 Developmental changes in behavioral performance

Results are reported when considering the population as a whole (group level), and when assessing individual longitudinal trajectories (individual level).

#### 2.5.2.1 Mean reaction time

##### *Group level*

Reaction time improved with age at the group level, qualitatively following and inverse age trajectory (t(1334)=9.033, p=5.7e-19). Group level interactions between age and the presentation interval (t(1334)=0.079, p=0.94) as well as delay interval (t(1334)=-0.12, p=0.90) were not significant .

##### *Individual level*

Developmental improvements in reaction time were also observable within individual developmental trajectories (t(1334)=7.68, p=2.98e-14. We did not observe a significant interaction between presentation interval and the within-subjects component of the inverse age term (t(1334)=0.71, p=0.47). However, in contrast to the group level results, we did observe a significant interaction between the within-subjects component of the

inverse age term and the duration of the delay interval (t(1334)=-5.31, p=1.35e-7), such that the effect of increasing the delay interval was greater in younger subjects.

#### 2.5.2.2 Accuracy

##### *Group level*

We observed improvements in group-level accuracy across development (t(1334)=3.04, p=0.0024), but did not observe and significant interactions between the group-level age regressor and the durations of the presentation interval (t(1334)=-0.072, p=0.47) or delay interval (t(1334)=0.036, p=0.71).

##### *Individual level*

We observed improvements in group-level accuracy across development (t(1334)=2.59, p=0.01), but did not observe and significant interactions between the group-level age regressor and the durations of the presentation interval (t(1334)=-1.28, p=0.20) or delay interval (t(1334)=-1.22, p=0.22).

#### 2.5.2.3 Reaction time variability

##### *Group level*

At the group level, reaction time variability decreased with age (t(1334)=7.55, p=8.0e-14). However, neither presentation interval nor delay interval terms showed significant interactions with group level age; (t(1334)=0.86, p=0.93) and (t(1334)=0.30, p=0.76) respectively.

#### *Individual level*

We observed a significant developmental reduction in reaction time variability at the level of the individual as well (t(1334)=6.95, p=5.73e-12). The interaction between individual level age trajectory and the length of the presentation interval was not significant (t(1334)=-0.76, p=0.44). However, as with mean reaction time, the interaction between delay interval duration and individual level age was significant (t(1334)=-3.7, p=0.0002), such that reaction time variability was reduced on long delay trials and the effect was more prominent when subjects were younger.

### 2.5.2.4 Precision

#### *Group level*

Like accuracy, the precision of memory-guided saccades improved with age, when observed at the group level (t(1334)=3.91, p=0.0001). Varying the presentation interval had no influence on precision and this absence of an effect was consistent across age (t(1334)=1.32, p=0.19). However, we observed a very modest but significant interaction between the length of the delay interval and group level age (t(1334)=-2.0, p=0.045) such that the precision of younger subjects saccades were less affected by changes to the delay interval.

#### *Individual level*

Age related improvements in precision were evident at the individual level (t(1334)=4.32, p=1.64e-5), but we observed no significant interactions between

individual level age trajectories and the presentation and delay intervals, ($t(1334)=0.025$, $p=0.98$) and ($t(1334)=-0.62$, $p=0.53$) respectively.

### 2.5.3 Intercorrelation of behavioral measures

All measures of behavioral performance were significantly correlated across sessions. Reaction time was positively correlated with reaction time variability ($r=0.699$; $p=1.2e-50$) and negatively correlated with accuracy ($r=0.14$; $p=0.012$) and precision ($r=0.28$; $p=2.18e-07$). As reaction time variability increased, accuracy ($r=0.13$; $p=0.13$) and precision ($r=0.35$; $p=2.05e-11$) tended to decrease. Lastly, greater accuracy was correlated with greater precision ($r=0.2$; $p=0.0002$).

### 2.5.4 Predicting age from behavioral measures

Given that mean behavioral performance was highly correlated with their corresponding measures of variability, we wanted to determine whether behavioral variability contributes additional information about the developmental status of a subject, beyond that contained in measures of mean behavioral performance. We compared the performance of linear models that predicted a subject's age from either their mean reaction times or accuracy to a matched linear model that contained the corresponding measure of behavioral variability. We quantified the significance of the comparison by using a simulated maximum likelihood estimation test with 1000 iterations. We found that a null model predicting age from only mean reaction time was significantly improved

by including reaction time variability as an additional parameter (null model: AIC=-2216.6, Log-Likelihood=1112.8; full model AIC=-2223.3, Log-Likelihood=1116.7; p=0.006). Predictions of subject age from accuracy were also improved by including variability, but this difference did not reach significance (null model: AIC= -2102.2, Log-Likelihood=1055.1; full model: AIC=-2103.3, Log-Likelihood=1056.6, p=0.087). These findings indicate that mean behavioral performance and behavioral variability each reflect important, and to some extent unique, aspects pertaining to the developmental state of a subject.

### 2.5.5 Characterizing the speed-accuracy relationship

An important aspect of behavioral variability is the relationship between the speed and accuracy of responses [31] —the speed-accuracy tradeoff. This relationship has been studied in the context of a number of different of behaviors and has provided important empirical support for computational accounts of perception, decision making, and response planning [33]. Like many rapid aimed movements, saccades also exhibit a speed-accuracy tradeoff. Research in this field has largely been aimed either at characterizing the psychophysical influences of features of saccade targets, e.g., size and distance from the current point of gaze [34], [35], or understanding computational mechanisms underlying visual search performance [36]. Developmental changes in the characteristics of the speed-accuracy relationship may provide insight into the mechanisms that support behavioral changes. However, to date, there is limited

published data characterizing the relationship between speed and accuracy for eye-movements made to single remembered targets in the absence of a visual stimulus.

For our analyses, we were only interested the behavioral variability observed within a particular session. Accordingly, we examined reaction time values, z-scored separately within the each of the four task conditions, and saccadic error, also z-scored and rectified within condition. In doing so, we ignored inter-subject and inter-session differences in behavioral performance, and limited ourselves to measuring trial-to-trial behavioral variability. We accounted for systematic differences in reaction time and accuracy arising from the spatial location of the targets by including each of the six possible target locations as a categorical nuisance regressor.

The association between reaction time and saccadic error exhibited a U-shaped relationship, in which there appeared to be two distinct regimes of speed-accuracy correlation (Figure 3): For roughly the fastest half of trials the expected speed-accuracy relationship prevailed, with faster trials being associated with greater saccadic error. However, for the slowest half of the trials, this relationship was strongly reversed with long latency trials exhibiting excessive saccadic error. Our regression analyses showed that saccadic error had a significant quadratic relationship with reaction time ($t(16362)=3.97$; $p=7.31e-5$), but no significant linear effect ($t(16362)=1.4$;$p=0.16$). We did not detect any main effects of or significant interactions with subject age (all $p > 0.1$) and therefore left age-related terms out of all regression analyses.

Next, we determined the proportion of trials belonging to each speed-accuracy trade-off regime by estimating the best fitting quadratic curve and calculating it's global minima, the point at which the direction of the speed-accuracy relationship reverses.

Comparing the location of the global minima against the empirical cumulative distribution of reaction times, we determined that approximately 52% of trials exhibited traditional speed-accuracy trade-off characteristics.

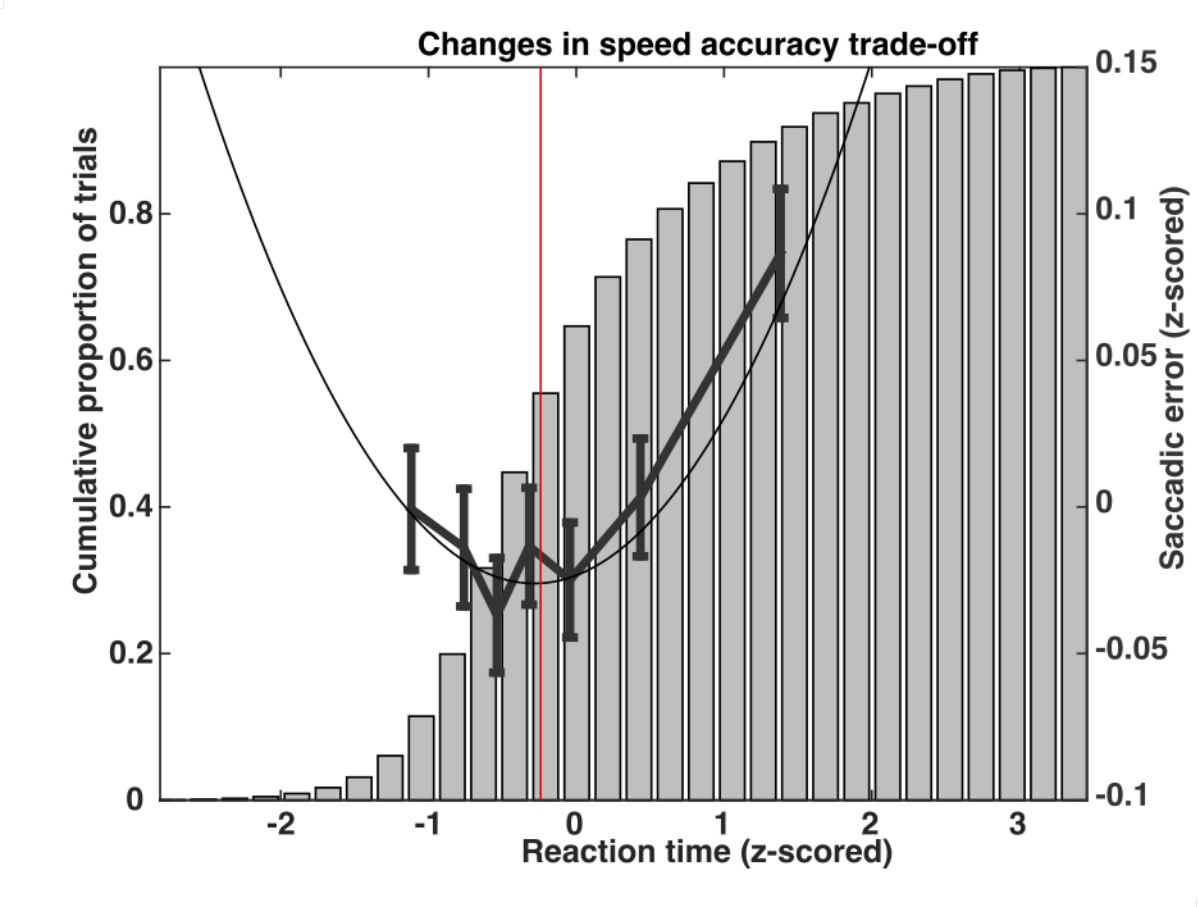


**Figure 3. Speed-accuracy relationship in the memory-guided saccade task**

**The U-shaped relationship between reaction time and accuracy in the memory-guided saccade task. The x-axis depicts reaction times, z-scored within a session. The left-hand y-axis is associated with the gray histogram, which depicts the cumulative distribution of trial reaction times. The right-hand y-axis is represents saccadic error, also z-scored within session, which is plotted in heavy black. Error bars represent one standard error of the mean. Behavioral data was adaptively binned so that each data point contains the same number of measurements. The smooth quadratic curve indicates the line of best fit**

**for the non-binned data. The vertical red line indicates global minima of the quadratic curve, the point at which the relationship between reaction time and accuracy changes direction.**

### 2.5.6 Independent trial-to-trial variability of threshold value and accumulation rate in a random walk diffusion model explains the speed-accuracy trade-off characteristics of the memory-guided saccade task

To understand the mechanisms underlying the peculiar U-shaped speed accuracy trade-off relationship, we turned to a class of stochastic accumulator models, which have been used to account for speed-accuracy relationships across response modalities. Typically, these models have been used to characterize behavioral performance in two-alternative perceptual decision tasks in which it is assumed that subjects base their choices on the stochastic accumulation over time of noisy sensory information [37]. In a common implementation of this model, two primary factors: the rate at which stimulus information accumulates and the threshold at which the subject deems it appropriate to initiate a response, determines reaction time, accuracy, and the relationship between them. For instance, changing response thresholds produces trials in which slower reaction times are associated with greater response accuracy —a traditional speed-accuracy relationship, qualitatively like that which is present on the left hand side of Figure 3**.** [38]. Trial-to-trial differences in accumulation rate produce a contrary relationship in which trials with slower reaction times tend to be least accurate

[39], like the right hand side. One goal for these simulations was to determine whether a balance might be struck between the two opposing influences of variable accumulation rate and response threshold to produce the observed U-shaped speed-accuracy relationship

Because of the binary nature of two-alternative forced choice tasks, the term “accuracy” in these models usually denotes the percentage of correct perceptual decisions rather than a continuous measurement of the magnitude of a response error. Here we describe a simple computational model of working memory retrieval processes which implements a version of the stochastic accumulation framework that is appropriate for characterizing data in which trial-to-trial error is a continuous variable (see Appendix B).

Memory-guided saccades are performed in the absence of visual input and are guided solely by a representation of the remembered location of the target, which is maintained in working memory. Producing a memory-guided saccade therefore would seem to involve some process in which working memory’s spatial information is transferred, or “read out”, into second pattern of motor-related neural activity that actually drives the production of the appropriate eye-movement. We operationally define the process of transferring information in working memory to a neural representation appropriate for generating motor commands as retrieval. It is this hypothetical retrieval transfer operation that we chose as our starting point for constructing the model.

In this computational model, spatial information is stored in working memory as a vector representation of the visual field sustained by the activity of groups of neurons. The vector of working memory neural activity is such that each entry represents a particular spatial location. In addition, the vector is ordered so that adjacent entries correspond to adjacent spatial locations. In this way, we model the representation of space in working memory in a manner not altogether different from how it is understood to be represented by the visual cortex at large. A remembered stimulus is encoded by heightened activity amongst the neurons representing the location in which it was presented (Figure 4**a**). We suppose that neurons representing adjacent spatial locations in the motor representation share some common inputs from the working memory representation. As a result, the read out, or mapping, of working memory to motor representations is somewhat diffuse and will be 'blurred' in the process of transferring to the motor representation (Figure 4**b**).

The actual read out of working memory information to a motor representation begins at the response cue. We model the transfer as an accumulation over time of the working memory representation into the motor representation, which is identically topographically organized. Two sources of random noise are considered to affect the transfer of information between representations. The first is trial-to-trial variability in neuronal gain affecting the amplitude of the representation in working memory (Figure 4**a-c**). Changes in working memory gain affect the rate at which the working memory representation accumulates, or is read out, into the motor representation. The second is independent random noise, due to background inputs, that accumulates within the activity of motor representation neurons (Figure 4**d**). Critically, we suppose that once

any single neuron in the motor representation vector reaches a predetermined threshold magnitude, a saccade is generated to the corresponding location. Trial-to-trial differences in the magnitude of the response threshold is a third source of variability, which does not affect the transfer of stimulus information, but changes the level of motor-related activity that must be achieved to evoke a response.

There are a several parameters that can be adjusted in this model. Among them are: 1) the width of the blurring, or the point spread function, that defines how diffuse the mappings are between working memory and motor representation; 2) the magnitude of the accumulating independent noise; 3) the mean value and variability of the threshold determining when a saccade is performed; 4) the mean value and variability of the gain modulations affecting the working memory representation. Although each of these parameters interact with one another in complex ways which warrant future exploration, here we explore the effects of potential developmental changes in the variability of the gain and threshold parameters, while holding their means along with all other parameters constant.

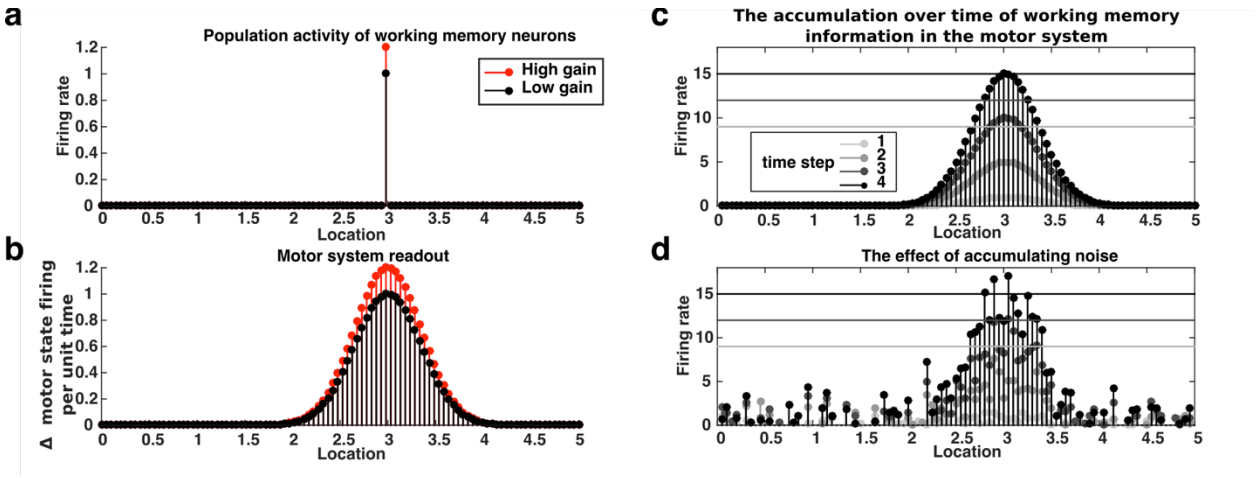


**Figure 4. Accumulation model of working memory retrieval**

**a) The firing rates of a hypothetical population of neurons that encode 1-dimensional spatial location in working memory. In this case, the pattern of activity indicates that the remembered target appeared at x=3. The red data points depict the pattern of activity that is present under conditions of increased neural gain affecting the working memory representation. b) The change per unit time in the state of the motor representation during the retrieval operation. The motor representation is a diffuse version of the working memory representation. On high gain trials (red) the accumulation of spatial information into the motor state happens much more quickly per unit time. c) During retrieval spatial information accumulates in the motor representation, increasing the activity of neurons that code for that location over time. The horizontal gray lines represent a variable firing rate threshold to execute a memory-guided saccade. d) Shows the effect of accumulating stochastic noise on the motor representation. Note that as the threshold gets higher, increasingly only neurons representing locations near the stimulus surpass it.**

For all simulations, we defined reaction time as the number of steps of accumulation that were required before one of the neurons in the motor representation reached the threshold. For each trial, the accuracy of the resulting simulated saccade was determined by calculating the distance between the location to which the saccade was generated, and the actual location of the target represented by working memory. To match our computational model to our task, we simulated 60 trials for each simulated subject, matching the number of trials that contributed to the z-scored session data.

Figure 5**a** depicts how trial-to-trial differences in the response threshold affects the speed-accuracy relationship, while holding all other parameters constant. When the only sources of variability are independent accumulation noise and trial-to-trial variability in the response threshold, we observe the typical speed-accuracy tradeoff relationship, where fast trials tend to be less accurate. To understand why this occurs, consider a trial in which the response threshold is low. In this case, very little neural activity within the motor representation needs to be accumulated before a saccade is triggered. This increases the likelihood that a random neuron, representing some location other than the correct target might accumulate to threshold simply by chance. At the same time, because the threshold is so low, the magnitude of neural activity required to trigger a saccade can be achieved very quickly. The combined effect is that trials with very fast reaction times, as a result of a low response threshold, are also those for which responses tend to be less accurate. On trials in which the threshold is high, a greater amount of time is required for neural activity to reach a magnitude sufficient to trigger a response. This increases reaction times. At the same time, the increase in response time allows the accumulated representation of the target location within the population of motor neurons to increase relative to the accumulated noise, ultimately making the saccade more accurate.

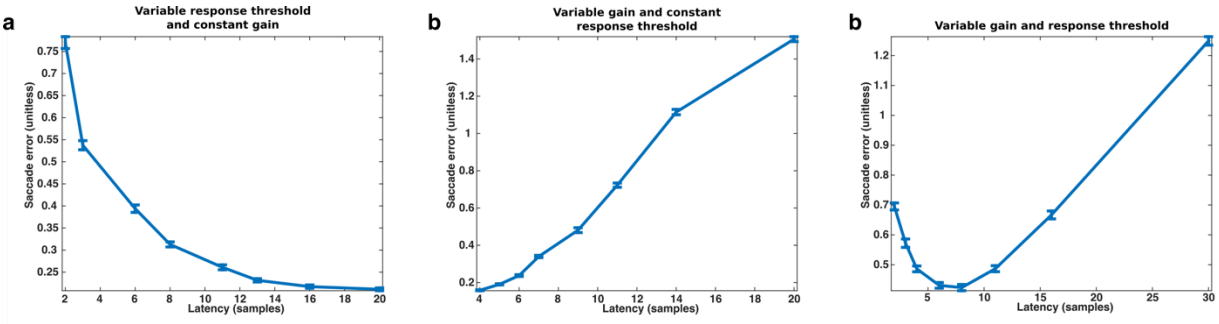


**Figure 5. Speed-accuracy relationships in the stochastic accumulator model**

**Each panel depicts the speed/accuracy relationship observed in our simulations. The x-axes indicate the simulated reaction time for a trial, given in terms of the number of accumulation steps that occurred before the response threshold was reached. The y-axes depict accuracy, measured as the absolute value of the difference in spatial location between the target and the actual saccade that was performed. a) Holding working memory gain constant across trials but allowing the threshold to vary, gives rise to the typical speed\accuracy relationship. b) The response threshold is fixed and working memory gain, and thus the accumulation rate, varies across trials. c) Both response threshold and gain fluctuate independently across trial within ranges that were determined, by a search of the parameter space, to qualitatively match the speed-accuracy relationship observed in our data**

Next, we examined what would happen if we allowed for trial-to-trial variability in the gain of the working memory representation, while holding the value of the response threshold constant. Here, we found that the relationship between reaction time and accuracy was reversed; trials with longer reaction times tended to be less accurate. In this case, when the response threshold is fixed, what dictates reaction time is the accumulation rate (Figure 5**b**). On trials where gain is high, the accumulation rate is also

high, leading to fast reaction times. Also, higher gain improves the signal to noise ratio of the working memory representation, minimizing the impact of noise and leading to more accurate saccades. These two effects lead to a tendency for faster saccades that result from high gain to be more accurate than slower saccades, a relationship opposite to what we observe with no gain modulation and a response threshold that changes across trials

Given that trial-to-trial variability in response threshold and gain modulation are predicted to induce opposing relationships between reaction time and accuracy, we set out to determine whether the two influences could be simultaneously present, and balanced in such a way as to account for the U-shaped speed-accuracy relationship that we observed in our behavioral data. To do this we performed a series of simulations in which we searched the space of model parameter values, to find whether we could qualitatively recapitulate the U-shaped speed accuracy curve observed in our data. In our parameter space search simulations, we allowed only the mean values and trial-to-trial variance of the threshold and gain parameters to vary, and held all other parameters, such as accumulation noise, number of neurons, and width of the point spread function, constant.

Figure 5**c** demonstrates that allowing independent trial-to-trial variability in response threshold values and working memory gain modulation is sufficient to account for the U-shaped speed accuracy trade-off observed in our data. In this case, parameter values were found such that the fastest trials are dominated by the effect of a response threshold, which changed across trials. Beyond a certain reaction time, however, increasing the response threshold yields diminishing returns on improving accuracy,

and trial-to-trial variability in working memory gain becomes the dominant factor in determining the speed accuracy trade off. The reason for this transition is that trials that have not reach the response threshold at this point tend to be those occurring when gain is low so that the motor representation is dominated by stochastic accumulated noise.

### 2.5.7 Coordinated changes in working memory gain and response threshold variability minimize developmental differences in the shape of the speed-accuracy tradeoff

Our simulations have shown that independent variability affecting working memory gain and motor response thresholds can account for the U-shaped speed-accuracy relationship that we observed in the memory-guided saccade task. However this speed-accuracy relationship was only apparent in normalized data, z-scored within a session, and did not exhibit any detectable age-related changes. Given that our analysis of empirical task behavior showed that mean performance and variability improved with development, our next goal was to reconcile our computational model with our behavioral findings. We therefore sought to determine whether coordinated changes in gain and response threshold variability could be made to simultaneously account for the known developmental changes in behavioral performance, while maintaining an age-invariant U-shaped speed-accuracy relationship.

We began with the set of model parameters found during our initial search of parameter space to produce a U-shaped speed-accuracy tradeoff. We then

systematically adjusted the parameters related to gain and response threshold variability, while holding all other parameters (including their mean values) constant. In this way, we searched a local region of parameter space, at each point estimating the mean and standard deviation of reaction time and average saccadic error. Additionally we estimated the shape of the speed-accuracy relationship by regressing trial-wise accuracy on reaction time, including linear and quadratic terms.

After each change in model parameters, we determined how similar the speed-accuracy relationship was to our empirical data by comparing the three-element vector of regression weights (constant, linear, and quadratic terms) from the simulated and empirical data. We summarized their differences by computing a “dissimilarity score”, given as the magnitude of the difference between both vectors. Smaller dissimilarity score mean that the empirical speed-accuracy relationship is more similar to simulated relationship. Figure 6**a** shows that a distinct path exists through parameter space (see Appendix B) in which coordinated changes in the variability of working memory gain and motor response thresholds minimize deviation from a U-shaped speed-accuracy relationship (Error! Reference source not found.**b**).

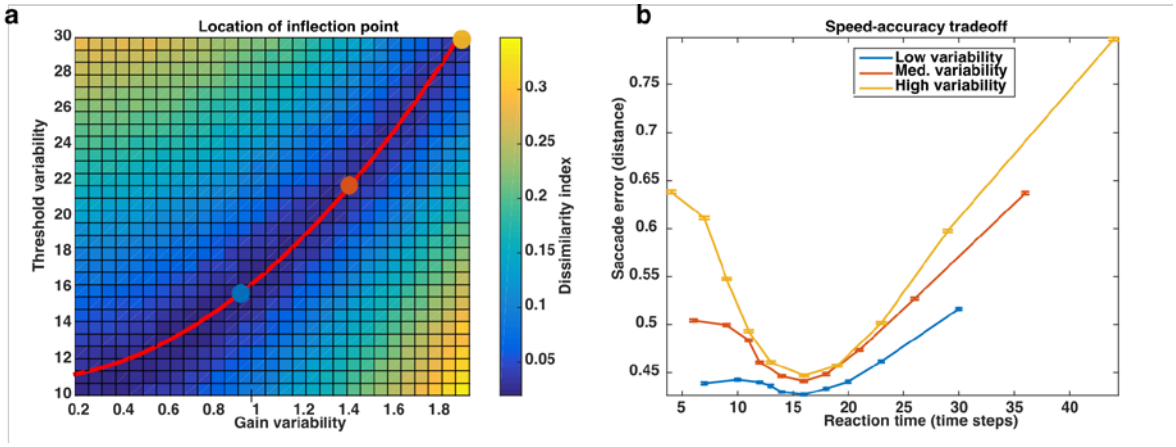


**Figure 6. Speed-accuracy gain and threshold variability parameter space**

**a) Dissimilarity index as function of gain variability and threshold variability. The dissimilarity index quantifies the difference between empirical and simulated speed-accuracy regression coefficients. Specifically, it is the magnitude of the difference between the vectors of the empirical and simulated speed-accuracy regression coefficients. The red line traces a trajectory through parameter space that minimizes the difference between empirical and simulated speed-accuracy relationship. b) Simulated speed accuracy relationships from the locations in parameter space indicated by the solid dots in (a). The x-axis represents reaction time as the number of drift steps before a threshold values was reached. The y-axis represents the average magnitude of the saccadic error. Error bars represent one standard error of the mean.**

### 2.5.8 Developmental reduction in gain and threshold variability can account for changes in behavioral performance during adolescence

We hypothesized that during adolescent development, both working memory gain and response threshold variability decrease in a coordinated manner, following a trajectory given characterized in Figure 6**a**. To determine whether such coordinated change in

variability could produce developmental changes in behavior that are consistent with what we observe empirically, we extracted estimates of mean reaction time and reaction time variability as well as saccade error from all point along the path and ordered them so that younger subjects were those with the greatest variability (Figure 7a-c).

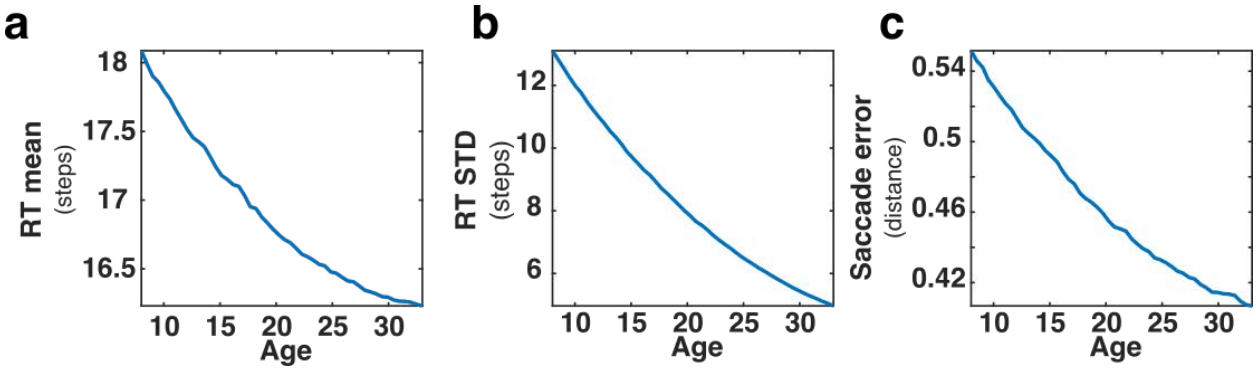


**Figure 7. Simulated developmental changes in behavioral performance**

**Model estimated changes in behavioral performance based on the assumption that response threshold variability and working memory gain variability decrease in a coordinated manner, minimizing age-related changes in the U-shaped speed-accuracy tradeoff. a) mean reaction time; b) standard deviation of reaction time; and c) mean saccade error —a proxy for saccade precision. The x-axis depicts subject's ages, which were arbitrarily scaled to match the age range of our data sample.**

We found that coordinated decreases response threshold variability and working memory gain variability could qualitatively account for the changes in behavioral performance that we observed during adolescence; all simulated measures of behavior improved following a curvilinear trajectory. As in the empirical behavioral data, we observed a greater fractional change in reaction time variability, compared to mean reaction time across development: simulated mean reaction time improved by roughly

10% compared to simulated reaction time variability which improved by roughly 60%. We also computed the average correlation between mean reaction time and reaction time variability for simulated sessions at 10 evenly spaced points along the putative developmental trajectory depicted in Figure 6**a** and found that, as with the empirical behavioral data, they were positively correlated (mean r=0.58; one-sample t-test: t(9)=15.5; p=8.46-e-8).

Lastly, we noticed that for simulated sessions with greater gain and threshold variability there tended to be a greater correlation between mean reaction time and the standard deviation of reaction time. This suggested to us that younger subjects in our data might likewise exhibit greater correlations between the means and standard deviations of their reaction times across sessions. To determine whether real behavioral data exhibited this characteristic, we divided our data into two groups by median split, and compared the correlation between the means and standard deviations of reaction time using a bootstrapping procedure. Consistent with our model predictions, we found that the correlation in the younger group (r= 0.713) was greater than the correlation in older group (r=0.573). We verified the significance of this age-related change by comparing the bootstrapped distribution of the difference between correlation coefficients between both groups (p=0.0024)

## 2.6 DISCUSSION

### 2.6.1 Developmental changes in behavior

Previous studies of developmental changes in memory-guided saccade performance used a version of that task that placed demands on response inhibition processes as well as working memory. Here, we demonstrate that developmental improvements in behavior during adolescence are still present after eliminating the demands on response inhibition. Our results indicate that developmental improvements in task performance are not simply the result of improvements in the ability to simultaneously balance working memory and response inhibition processes.

Differences in the amount of time that subjects were allowed to look at the target, the presentation interval, did not significantly alter any aspect of behavioral performance. We had hypothesized that increasing the amount of time that subjects were allowed to look at, or "encode" the location of a target would improve the fidelity of its representation in working memory, possibly improving the accuracy and reaction time of responses. We infer from the absence of any measurable effect of increasing the presentation interval on any aspect of behavioral performance, that the encoding of spatial information occurs on time scales faster than 1.5 seconds for all ages under study.

Reaction times were generally faster and less variable during in long delay interval trials. This difference may arise either from allowing a subject a greater amount of time to prepare their saccadic responses, or perhaps as a result of the reduction in

uncertainty in the exact time that a response is required for long delay trials. That is, during short delay trials, in the moments right before the response cue, subjects do not know whether the trial contains a short or long delay interval. During long delay trials, once, the initial 1.5 seconds has elapsed without the appearance of a response cue, subjects may infer exactly when the response cue will appear, since the only other option for delay is 9 seconds. Greater uncertainty about the required timing of a memory-guided saccade may increase reaction time. That the facilitating effects of increasing the delay interval were more pronounced in younger subjects, indicates that adult behavior is affected less by uncertainty in the response time.

One way to interpret the high degree of intercorrelation between all of the measures of behavioral performance as well their similar developmental trajectories is that all aspects of behavioral performance are influenced by the same beneficial developmental changes in the underlying cognitive and sensorimotor systems that support task performance. However, our finding that reaction time variability significantly improved prediction of subject ages over mean reaction time indicates that behavioral variability does capture some unique features of developmental change. This could happen if developmental changes in average reaction time were influenced by developmental factors that do not affect reaction time variability. The continuing myelination of long distance projections, which increase the average rate that information is transmitted and processed [40] might influence mean reaction time, while differences in reaction time variability might be the result of changes in stochastic neural variability which also improves in parallel during development and is associated with behavioral variability [14], [15].

### 2.6.2 Computational insights into the development of working memory performance

Our simulation studies provide insight into the possible neural mechanisms yoking developmental changes in mean behavior and behavioral variability. We found that a simple high-dimensional extension to the drift diffusion modeling framework could account for the seemingly age-invariant U-shaped speed-accuracy relationship that we observed for memory-guided saccades. In this model, the processes involved in producing a memory-guided saccade are approximated as the drift diffusion of a topographic working memory representation into a similarly topographic oculomotor representation, which, upon reaching a threshold value, evokes a saccade. The maintenance of a U-shaped speed-accuracy tradeoff was found to require a balance between two independent sources of variability that affect the gain of a working memory representation and the response threshold at which an oculomotor responses is evoked.

We found that reducing the magnitudes of independent gain and threshold variability in concert produces changes in behavioral performance that share several features with the developmental changes in behavior that we observe empirically. Specifically, we found that stabilizing working memory gain and response threshold variability produces curvilinear changes in average reaction time, reaction time variability, and saccadic error, which are qualitatively similar to true developmental data. We therefore propose that the stabilization of working memory gain and oculomotor

response thresholds may be a key factor in the developmental improvements in mean behavior and behavioral variability.

Although our model is agnostic about the exact anatomy in which it is instantiated, other experiments offers suggestions about it may be implemented in the brain. As noted earlier, working memory representations appear to be widely distributed across cortex, mainly within the regions that represent the corresponding sensory modalities that are being remembered [21]. Thus, the working memory representation in our model is likely to have many contributing support regions. The superior colliculus, containing neurons whose activity represents a retinotopic map of saccadic trajectories, is plausible site for the instantiation of the motor representation of our model [41]. Reducing in GABAergic input from the substantia nigra to the superior colliculus results in changes in saccade metrics that are particularly pronounced for memory-guided saccades and consistent with the lowering of a response threshold [42]. The role of GABA in setting a response threshold is also strongly suggested by simulations studies of cortico-striatal-collicular interaction [43]. A variety of mechanisms may contribute to modulation of gain signals affecting working memory. For instance, cortical gain is affected by a variety of cognitive and biophysical processes. Norepinephrine [44], acetylcholine [45], and dopamine [46] are known gain modulators implicated in arousal and the allocation of spatial attention; indeed, simply changing the levels of background synaptic input can alter neuronal gain [47]. These critical neurotransmitter systems may be undergoing important specialization through adolescence as adult level function is being established resulting in greater stability through development.

# 3.0 DEVELOPMENTAL DIFFERENCES IN WHOLE BRAIN GAIN STABILITY

## 3.1 BACKGROUND

### 3.1.1 Relating brain activity and behavior

Humans and animals can rarely perform a particular behavior many times in exactly the same way. Our analyses of performance during the memory-guided saccade task indicate that instability in behavioral performance is more pronounced in younger subjects and decreases during adolescence. Experiments have shown that subtle differences in behavior covary with the activity of individual neurons, groups of neurons, and whole brain regions thought to be involved in task performance [48]-[51]. In regions of visual cortex for instance, neurons do not respond identically to repeated presentations of the same stimulus. Such trial-to-trial variability in neural responses is thought to underlie fluctuations in behavioral performance that occur during visual perception tasks that rely on information represented by visual cortex [48].

Theoretical analyses indicate that in order for there to be measureable trial-wise correlations between individual neurons and behavioral performance, one of two things must be true: either very few neurons contribute to the behavior —on the order of a few dozen— or the activity of the neurons contributing to the behavior must be correlated

[52], [53]. The reason for this, intuitively, is that when many uncorrelated neurons contribute to behavior, the contribution of any one neuron is washed out amidst the welter of contributions from the other neurons. However, when the activity of many neurons driving a behavior is correlated, variability affecting one neuron is partly reflected in the activity of all neurons, amplifying the effect on behavior and imposing on it a trial-to-trial relationship with the activity of individual neurons.

Recent fMRI data has suggested that even very simple tasks involve activity that is distributed across most of cortex. Gonzalez-Castillo and colleagues had subjects perform many hundreds of trials of a simple letter/number discrimination task in an fMRI scanner. With a sufficient number of trials present to counter measurement noise, they found that the vast majority of cortex exhibited task-locked BOLD responses [54]. Assuming that neural variability is mainly independent across brain regions, their result would predict that the trial-to-trial relationship between the activity of any particular region and behavior would be minimal. However, the combined activity of many neurons within a single brain area can be used to predict trial performance with high accuracy. Cohen and others provided a striking example of this in an experiment showing that performance on a change detection task could be predicted with very high accuracy by examining the activity of a few dozen simultaneously recorded neurons in visual area V4 [49]. One way to reconcile these two findings is to propose that neural variability across brain regions is correlated, and that many brain regions exhibit the same trial-to-trial fluctuations in neural responses that predict behavioral performance.

The correlated neural variability associated with trial-to-trial fluctuations in task performance is likely to arise from multiple sources including stochastic variability

occurring within shared bottom-up inputs into sensory cortex [52] and the widespread coherent fluctuations of brain activity, of the type examined in resting state studies [55], [56]. Somewhat more recently though, experiments have demonstrated that trial-to-trial variability in top-down signals, likely related to attention, are a major contributor to correlations between neural activity in sensory cortex and behavior [49], [57], [58] .

Attention is known to primarily affect the gain of neural responses [59], [60]. The hallmark of gain modulation is a multiplicative scaling of neural activity that does not alter the shape of neural tuning curves, or the spatial distribution of activity. A key feature of neuronal correlations induced by instabilities in attention is that their structure is consistent with fluctuations of shared gain modulation [61]. That trial-to-trial fluctuations in gain signals are associated with behavioral instability is consistent with our computational modeling analysis of memory-guided saccade task performance; Our results suggest that the improvements in behavioral variability as well as mean behavioral performance may be driven, in part, by the stabilization of gain signals affecting working memory representations.

Combined, this evidence suggests that gain modulation may play two important roles: 1) producing trial-to-trial differences in behavioral performance by altering the magnitude of neural responses across trials; and 2) providing a source of correlated, and potentially widespread, neural variability that allows for trial-to-trial correlations between neural activity and behavior to be observed at all.

For these experiments, we sought a BOLD signal-based metric of trial-wise gain modulation. We hypothesized that variability in gain would result in fluctuations in the amplitude of expression of whole-brain patterns of task-related BOLD signal, or what we

refer to as *brain state variability*. Furthermore, we hypothesized trial-to-trial differences in behavioral performance would be correlated with brain state variability, and that that the developmental stabilization of behavior that we observed would be associated with a reduction in brain state variability as gain signals similarly stabilize during adolescence.

## 3.2 METHODS

We supposed that brain state variability, or trial-to-trial differences in the amplitude of patterns of task-related BOLD signal, would be related to trial-to-trial changes in behavior. Here we present an outline of the procedure used to define task-related brain state patterns (for complete details see Appendix). To determine what patterns of activity were associated with visuomotor/encoding (VME), working memory maintenance, and retrieval processes that support performance of the memory-guided saccade task, we extracted representative spatial patterns of BOLD signals from different periods of the average time courses of the long delay trials. To represent VME and retrieval processes we extracted the pattern of BOLD signals occurring 6 seconds after the visually-guided and memory-guided saccades, which allowed the signals associated with these processes to reach their peak [62]. The pattern of activity associated with working memory maintenance was extracted from the TR immediately prior to the execution of the memory-guided saccade. Implicit in this procedure is the assumption that VME, maintenance, and retrieval processes are associated with distinct

and consistent patterns of whole-brain BOLD activation that are expressed with the time course of a hemodynamic response. We orthogonalized each of the brain state patterns to ensure that they captured unique aspects of task activity by regressing the VME-related pattern from maintenance-related pattern, and regressing both VME- and maintenance-related patterns from the retrieval related pattern. This process removed remaining components of VME-related activity from the maintenance activity and importantly, allowed us to remove the pattern of activity associated with visuomotor responses from the retrieval-related pattern. Evidence suggests that some known neuronal gain modulators, particularly those acting through cholinergic pathways, specifically alter gain with hemispheric specificity, similar to the effects of directed spatial attention [45], [63], [64]. Accordingly, we decomposed each of the three resulting whole-brain patterns into hemifield-specific, or “spatial”, and hemifield-non-specific, or “mean”, brain state components. These brain states reflect the engagement of canonical regions underlying the VME epoch (e.g., frontal eye fields), maintenance (e.g., prefrontal and frontal eye fields), and the non-visuomotor aspects of retrieval (e.g., preSMA) (Figure 8).

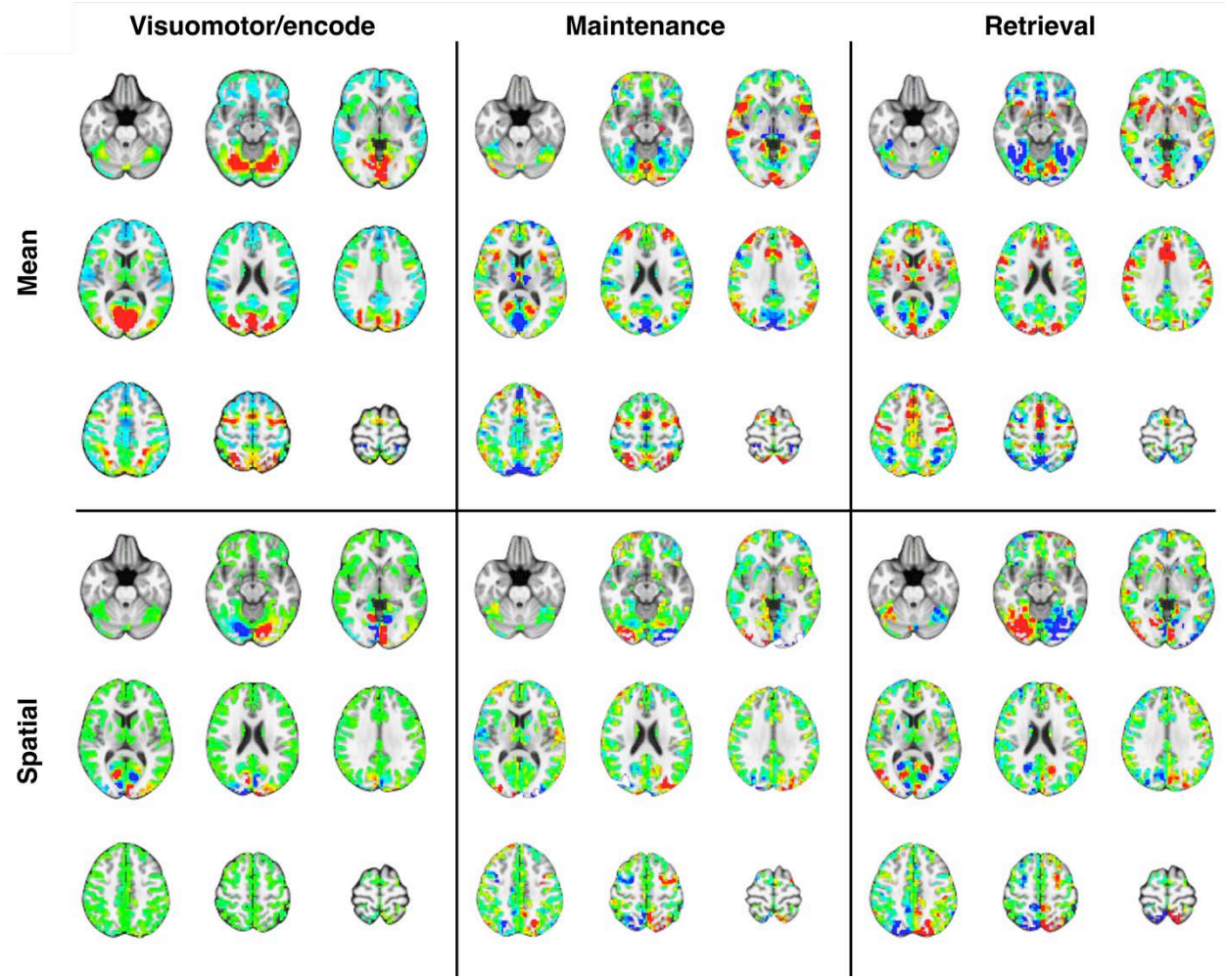


**Figure 8. Components of task-related brain states**

**Mean, or spatially non-specific (top row) and spatial (bottom row) brain state components. All brain state component patterns have zero mean across voxels and have been normalized to a common vector magnitude. Red indicates regions with the greatest activity within a state, blue indicates regions with the least, and green the regions with the smallest contributions to the state.**

## 3.3 RESULTS

### 3.3.1 Task-related brain states are expressed similarly across age

After constructing the set of task-related canonical brain state patterns, we verified that whole brain trial-locked BOLD activity could be sensibly characterized as separate time courses of their superimposed expression. For instance, to be considered sensibly expressed, the VME state components, intended to represent the whole brain pattern of activity evoked by a saccadic eye movement, should exhibit two peaks of expression during the average (long delay) trial: once following the initial encoding saccade and again following the memory-guided saccade. The mean maintenance state, to the extent that it represents activity associated with sustained spatial working memory and saccadic preparation, should exhibit a prolonged time course, rising after the first visually-guided saccade and peaking near the time of the memory-guided saccade. The retrieval state, intended to represent the pattern of activity associated with the production of an endogenously guided saccade, after removing the component of activity associated with the eye-movement itself, should be expressed only following the production of the memory guided saccade.

Our expectation for the time courses of the spatial brain state components are somewhat more nuanced due to the fact that visual and oculomotor processes (and, of course, sensorimotor processes in general) are distributed in a hemisphere-specific way across the cortex. We expected therefore that aspects of the VME, maintenance, and retrieval states should differ systematically depending on the visual hemifield in which a

target appears. The spatial components of each brain state, defined as the difference between brain state patterns for right- and left-side visual targets, are meant to capture these differences. We expect not only that they be expressed at the appropriate times associated with the appropriate task epochs, like the mean brain state patterns, but that the sign of their expression should differ depending on the location of the visual target. Specifically, because the spatial states were constructed by subtracting left side patterns from right side patterns, we required the spatial state to be expressed positively for trials in which the target was in the right visual hemifield and negatively for targets on the left.

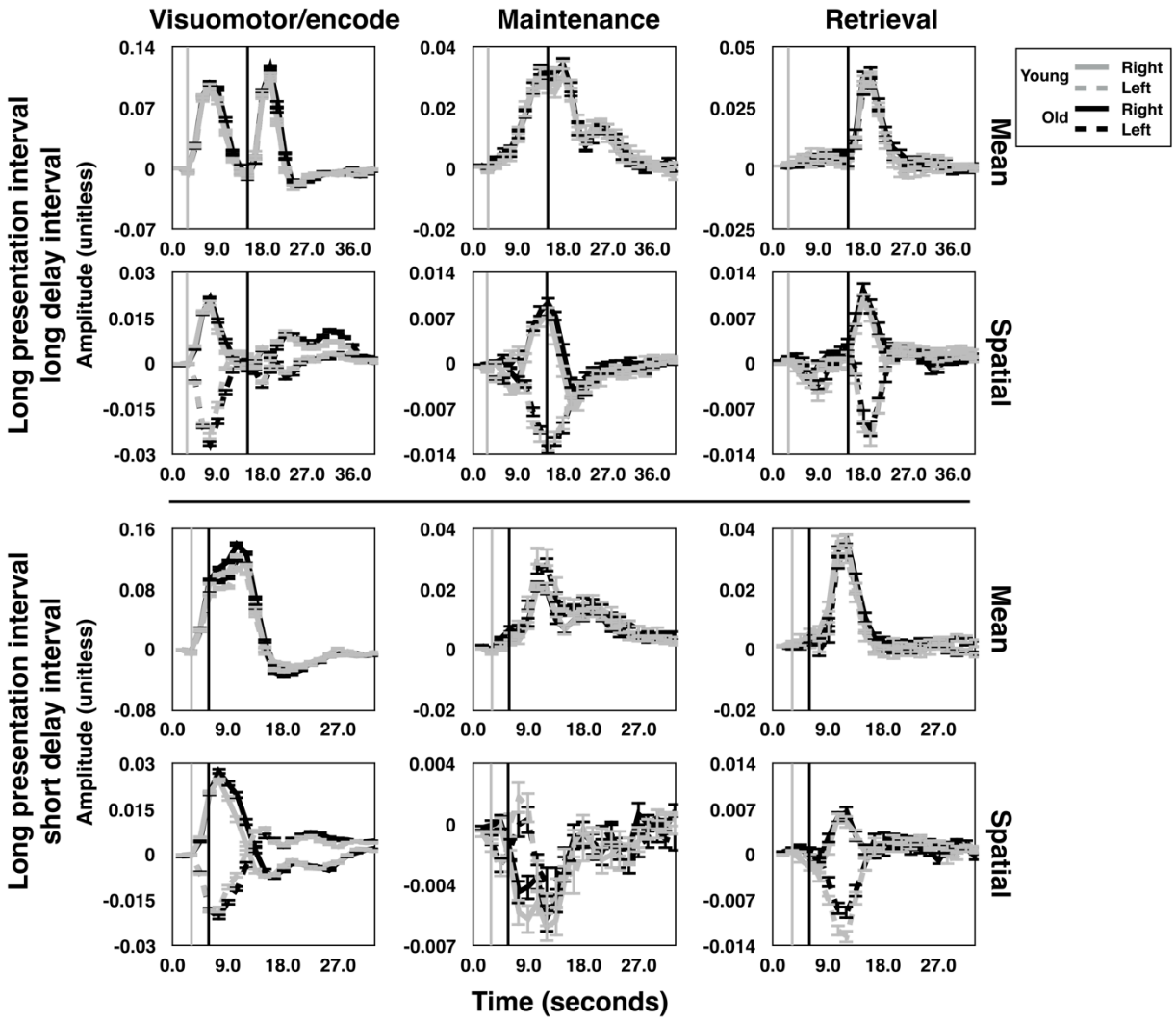


**Figure 9. Time courses of brain state expression for two types of trials**

**The average time courses of expression for each brain state component during long presentation long delay trials (top subset) and short presentation short delay trials (bottom subset). Each panel depicts the average time courses for the oldest (grey lines) and youngest (black lines) halves of the subject pool. The time courses for trials during which targets were presented in the left (dashed) and right (solid) visual hemifields are rendered separately. The grey and black vertical lines indicate the time of visually-guided**

**and memory-guided saccade signals respectively. Error bars depict one standard error of the mean.**

To test these suppositions, we converted the average whole brain time course for each type of trial into a time course of brain state expression by projecting each TR onto the complete set of brain state patterns using linear regression. For each brain state component, we constructed time courses of expression using the regression coefficients estimated at each TR. We submitted each brain state component's time courses for left and right side targets, separately for each trial type, to a linear-mixed effect analysis in which we modeled its expression over time in the following way:

$$\boldsymbol{Expression(TR) \sim TR * Target * Age + TR * Target * Displacement + (1|ID)}$$

**Equation 2. Brain state expression by time model**

Where:

- **I.** $Expression(TR)$ refers to the projection of the whole brain time series for a given type of trial onto a brain state pattern at a particular $TR$.
- **II.** $TR$ is a categorical variable representing each time point in trial time course.
- **III.** $Age$ refers to the age of a subject during a particular session
- **IV.** $Target$ is a dummy-coded regressor (-1 or 1) indicating whether the projection value was observed during right or left side trials
- **V.** $Displacement$ is a measure of the average per frame Euclidean displacement undergone by a subject during the session.

This model allowed us to estimate the average time course of expression for each brain state component while also measuring any systematic temporal variations arising from age-related differences, target hemifield effects, and in-scanner motion.

We confirmed that the expression of every brain state component significantly changed during each trial type (all $p < 0.001$), using separate omnibus F-tests, which tested the null-hypothesis that all of the coefficients for TR and TR•Target terms are equal to zero. As expected, we found that the mean and spatial components of each brain state pattern were expressed at the appropriate time during the trial, demonstrating that these canonical brain state patterns served as an effective condensed basis for characterizing the whole-brain patterns of BOLD activity across subjects. Additionally, the brain state patterns, which were derived from the long delay trials, generalized to an effective basis for describing BOLD activity evoked by short delay trials, which had markedly different task epoch timing **(**Figure 9 lower panel)

Next, we looked for age-related differences in the time courses of expression of the brain states across time for each trial type. Again, we applied an omnibus F-test to assess the null-hypothesis that all of the coefficients for Age•TR and Age•TR•Target were equal to zero. We observed significant age-related differences in the time courses of expression for the spatial, but not mean, component of the VME states across all trial types (all $p < 0.001$). We did not detect any significant age-related differences in the expression of either mean or spatial components of the maintenance state (all $p > 0.12$). Result for age-related differences in the time courses of expression for the retrieval states were mixed: We observed no omnibus age-related differences within either of the long delay conditions, but within the long presentation interval/short delay interval trials we observed a small age-related difference in the expression of the spatial retrieval state ($F(42,14652)=1.5$; $p=0.017$). Post-hoc examination of the individual Age•TR and Age•TR•Target coefficients at each time point in the trial revealed that this effect was

driven by slightly greater expression of the state by adults, across right and left side targets, during the 5th, 6th, and 8th TRs. However, in our post-hoc analysis no single time point reached significance (minimum(p) = 0.055). We also observed that the mean retrieval state was differentially expressed across age within the short presentation/long delay interval trials ($F(40,13986)=2.0$; $p<0.001$). Post-hoc analyses revealed that this effect was driven by a slightly greater expression of the mean retrieval state by adults during this condition during the 9th-12th TRs, well after the occurrence of peak expression for this state.

From visual inspection it is clear that adults exhibit a prolonged expression of the spatial component of the VME brain state during the different trials. We also wanted to know whether the peak amplitude of spatial VME expression differed with age. From each session we examined the amplitude of peak expression of the spatial VME state for each trial type. Because the sign of expression of the VME state varies depending on target hemifield, we extracted the maximum value of positive expression for right side trials, and we extracted the minimal value of expression for left side trials, and applied the following model for analysis:

$$\boldsymbol{Peak\ expression} \sim \boldsymbol{Condition} * \boldsymbol{Target} + \boldsymbol{Age} * \boldsymbol{Target} + \boldsymbol{Displacement} * \boldsymbol{Target}$$
$$+ \boldsymbol{VGSCorrect} * \boldsymbol{Target} + \boldsymbol{MGSCorrect} * \boldsymbol{Target} + (\mathbf{1}|\boldsymbol{ID})$$

**Equation 3. Peak brain state expression model**

Where:

**I.** $Peak\ expression$ refers to the magnitude of maximal (positive or negative, depending on target hemifield) expression of the spatial VME brain state

II. $Target$ is a dummy coded (-1 or 1) variable indicating the visual hemifield of the target

III. $Condition$ is a categorical variable referring to one of the four task conditions

IV. $Age$ refers to the subjects age at the time of measurement

V. $Displacement$ is the average Euclidean displacement per TR within the scanner.

VI. $VGSCorrect$ and $MGSCorrect$ indicate the percentage of trials during a session for which eye-tracking quality was sufficient to determine that the visually- and memory-guided saccades were performed correctly.

If adults expressed the spatial VME state to a greater extent than children and adolescents, this would result in greater positive expression for right side trials and reduced (more negative) peak expression during left side trials. We therefore examined the Age*Target interaction term, which we found did not reach significance (t(2672)=1.79; p=0.074). However, we did note that excessive motion was strongly associated with reduced peak expression of the spatial VME component (t(2672)=-7.68; p=3.14e-22).

Combined, these results demonstrate that the set of brain state patterns provide a simplified low dimensional basis for describing BOLD signal changes evoked by the memory-guided saccade task. Importantly, age-related differences in the expression of the brain state patterns during task performance were minimal, and only the spatial component of the VME state exhibited consistent age-related differences in expression across trial types. Even here, however, the age-related differences were not ones of magnitude, but of duration.

### 3.3.2 Trial-to-trial variability in brain state expression predicts behavioral performance

We hypothesized that trial-to-trial differences in behavioral performance may be caused by transient fluctuations in global gain signals occurring around the time of a behavioral response. Since variability in global gain signals are expected to amplify or attenuate ongoing patterns of task-evoked activity without changing their spatial structure, we predicted that reaction time and saccadic error would co-vary with the amplitude of expression of whole-brain patterns of task-related BOLD activity.

To measure the fluctuations in brain state expression, we examined the whole brain residual BOLD signal time series, which, after removing the mean trial responses from each voxel, represent inconsistent neural signals that are not synchronized with the task, as well as other biological and non-biological nuisance artifacts. We projected the spatial pattern of BOLD signal residuals from each TR onto the set of canonical brain state patterns (for complete details of this procedure, refer to the Appendix). The resulting regression weights associated with each brain state component, organized into a time series, are time courses of brain state variability, revealing whether a particular brain state pattern was present more or less than average at each TR; A positive regression weight at a particular TR indicates greater than average expression, predicted to be associated with high global gain, and a negative value indicates less than average expression, associated with low gain.

Within the time series of brain state variability, we determined whether there was a specific time interval around each memory-guided saccade in which trial-to-trial

fluctuations of the expression of the states were associated with differences in behavioral performance. To do this, we extracted snippets from the time series of each brain state component, centered on the TRs containing each correct memory-guided saccade and extending ±15 TRs before and after, and aligned them. We then performed a series of regression analyses, using brain state variability estimates from each relative TR, to determine the relationship between the expression of the states and reaction time and accuracy (saccadic error) of the memory-guided saccades. At each relative TR, we compared the results of a regression model that included only non-neural predictors of behavioral performance (a null model) to a second regression model that contained additional terms reflecting the brain state expressions at the TR being analyzed.

$$Behavior(trial) \sim Target + Eccentricity^2 + Run * TrialNumber + BehavioralCovariate + (1|ID)$$

**Equation 4. Null model for trial-wise brain state and behavior analysis**

Where:

**I.** $Behavior(trial)$ is either reaction time or accuracy of a saccade for a particular trial

**II.** $Target$ is a dummy coded regressor (-1 or 1) indicating whether a target appeared on the left or right

**III.** $Eccentricity$ is an integer, 1-3, with larger numbers indicating more eccentric target locations

**IV.** $Run$ is an integer, 1-3, representing the which of the three runs contained the trial

**V.** $TrialNumber$ is an integer, 1-20, indicating which trial within a run the behavioral measure came from

VI. $BehavioralCovariate$ is the value of the other behavioral measure not being directly analyzed. For instance, when modeling reaction time, accuracy is included as a covariate and vice versa.

$$\boldsymbol{Behavior(trial) \sim Target + Eccentricity^2 + Run * TrialNumber} + \boldsymbol{BehavioralCovariate + VMEMeanProjection(TR)} + \boldsymbol{VMESpatialProjection(TR) * Target + MainMeanProjection(TR)} + \boldsymbol{MaintSpatialProjection(TR) * Target} + \boldsymbol{RetrievalMeanProjection(TR) + RetrievalSpatialProjection(TR) * Target + (1|ID)}$$

**Equation 5. Full model for brain state and behavior analysis**

Where (considering just the terms that distinguish the full and null models):

I. $* Projection(TR)$ is the regression coefficient for a particular brain state component (mean and spatial VME, maintenance, and retrieval) taken from a given TR relative to the memory-guided saccade in question

Figure 10 depicts the results of these analyses performed at each relative TR and demonstrates that trial-to-trial variability in both reaction time and accuracy are related to fluctuations in the expression of task-related brain states occurring around the time that the memory-guided saccade was executed. For trial-wise reaction time, brain state/behavior associations were significant beginning with the TR when the memory-guided saccade was executed, peaking 1 TR after the saccade and lasting for a total of 6 TRs. Within this range, trials with faster reaction times were associated with greater early expression of the mean VME and maintenance brain states (TRs 0–2), and reduced later expression of all mean states (TRs 3–5). Trials with faster reaction times

were also associated with greater expression of the hemifield-appropriate spatial VME (TRs 1–3), maintenance (TR 2), and retrieval (TRs 1–2) states. The greater early expression and reduced later expression of the mean brain states for fast reaction time trials (represented by the transition from blue to red in some rows of the lower panel of Figure 10**)** is consistent with a simple correlation between the timing of a saccade and the latency of the expression of the brain state. We therefore performed a set of simulations to compare the temporal patterns of BOLD signal residuals for fast and slow reaction time trials that would result from latency-, amplitude-, and latency and amplitude-based relationships. We found that the trial-wise relationship between reaction time and the expression of the mean VME brain state was inconsistent with both a purely amplitude-based mechanism, and purely latency-based mechanism and instead reflects a mixture of the two effects (see Appendix D).

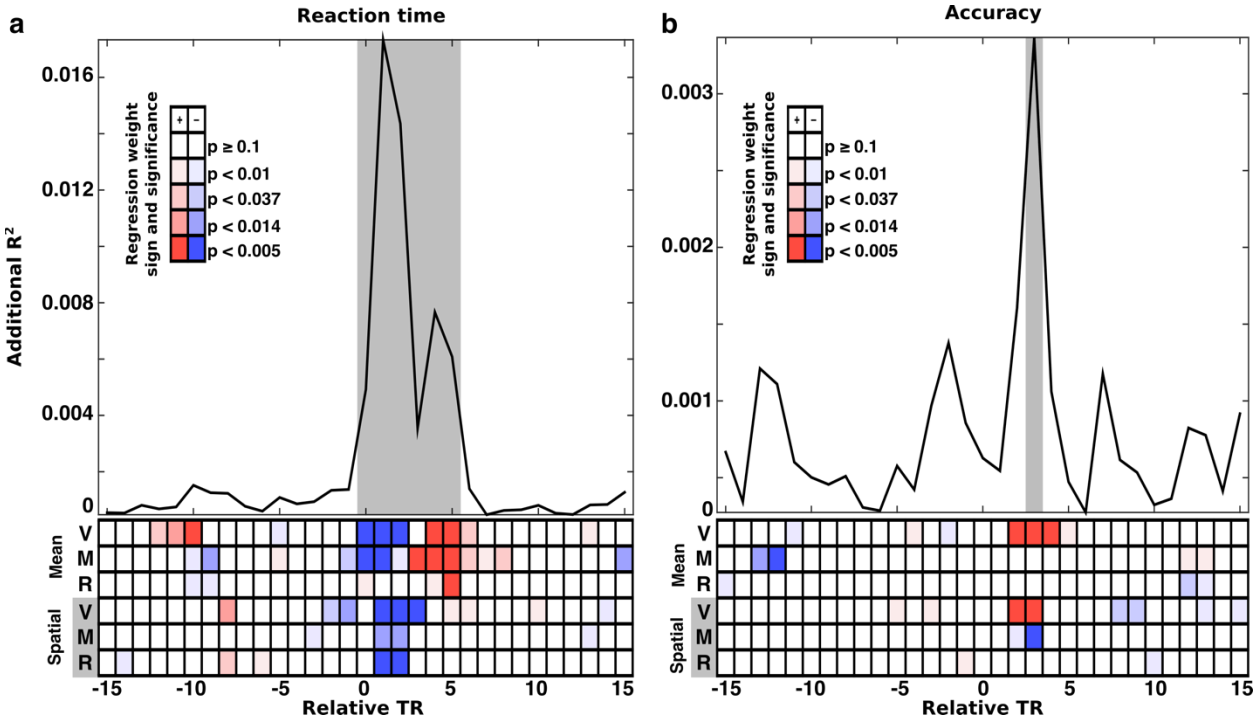


**Figure 10. The trial-wise relationship between brain state expression and behavior**

**Trial-to-trial fluctuations the expression of task-related brain states is associated with reaction time (a) and saccade error (b). The top panels depict the additional fraction of behavioral variability (compared to a null model) accounted for by including brain state measurements from each TR relative to each correct memory guided saccade. The null model, against which the full brain state model was compared, included the non-neural trial-to-trial covariates such as target location and its square and task condition. The null model for trial-wise reaction time included saccade error and its square as regressors. Similarly, the null model for trial-wise accuracy included reaction time and its square. Highlighted grey intervals represent TRs where the full models provided better a better fit than the null model (simulated likelihood ratio test with 5000 iterations; $p<0.001$). Each cell in the lower panels of (a) and (b) represent the p-value (darker colors are more significant) and the sign of the regression coefficient (blue, negative; red, positive) for each brain state component. The top three rows of cells represent the mean brain state components (V: VME; M: maintenance; R: retrieval). The bottom three rows represent the significance of interactions between the spatial brain state component and the target hemifield.**

The relationship between trial-wise accuracy and brain state expression was similar, but less prominent, and significantly present during only the 3rd TR following the MGS. At this time, when the mean and spatial components of the VME brain state were highly expressed, the accuracy of the saccade was worse (increased saccadic error). At the same time, greater expression of the target-hemifield-appropriate spatial maintenance brain state was associated with more accurate memory-guided saccades.

We noted that greater expression of VME brain states was associated with faster reaction times and reduced accuracy. This relationship, particular to VME, prompted us to examine the behavioral data for signs of a speed-accuracy trade-off. We found a significant quadratic relationship between z-scored reaction time and saccadic error at the trial level indicating that, within each session, excessively fast and slow responses were associated greater saccade error ($p=0.0008$).

### 3.3.3 Brain state variability decreases with age

After finding that trial-to-trial variability in the expression of task-related brain states was associated with behavioral variability, we explored the possibility that the developmental reduction in behavioral variability that we observed in the trajectories of task performance was the result of stabilizing global gain signals. To test this hypothesis, we first needed to establish whether a relationship between brain state brain state variability and age existed, and determine whether the magnitude of brain state variability decreased during development.

For each session, we computed the proportion of whole-brain BOLD signal variability associated with trial-to-trial fluctuations in the combined expression of the task-related brain states (see Appendix). We considered only BOLD signal variability occurring within the time interval around each memory-guided saccade found to be significantly related to behavioral variability (0–5 TRs), submitting this data to a linear mixed-effects analysis by applying the model:

$$\boldsymbol{BrainStateVariability} \sim \boldsymbol{FirstVisitAge} + \boldsymbol{RelativeAge} + \boldsymbol{Displacement} + \boldsymbol{MotionVariance} + \boldsymbol{SessionMeanPercentCorrect} + (\mathbf{1} + \boldsymbol{RelativeAge}|\boldsymbol{ID})$$

**Equation 6. Total brain state variability age model**

Where:

**I.** $BrainStateVariability$ is the proportion of BOLD signal variability, occurring in the 0-5 TR window around each memory guided saccade, that corresponds to brain state variability

**II.** $FirstVisitAge$ is the age of a subject at their first session. This term is used to model the group-level age trajectory.

**III.** $RelativeAge$ is the time between a subjects' first session and each subsequent session, a term that models the slope of individual trajectories.

**IV.** $Displacement$ is an estimate of average Euclidean displacement in the scanner

**V.** $MotionVariance$ is a secondary measure of the magnitude of residual motion-related BOLD signal artifacts (see Appendix for details)

**VI.** $SessionMeanPercentCorrect$ is the percentage of trials during which eye-tracker performance allowed us to determine the latency and accuracy of both visually- and memory-guided saccades.

**VII.** $(1|RelativeAge|ID)$ are mixed-effects terms that account for the longitudinal nature of the data by modeling a random slope and offset for each individual subject

We found that brain state variability significantly decreased with age at the group level (t(330)=-3.35; p=9.0e-4). However, the term for individual-level change did not reach significance (t(330)=-1.6; p=0.11). Neither in-scanner displacement nor degrees of residual motion artifacts were significant predictors of brain state variability in this model ((t(330)=-0.15;p=0.88) and (t(330)=0.53; p=0.59) respectively). We also observed

that brain state variability was higher in subjects who had performed fewer correct trials ($t(330)=-3.14$; $p=0.002$).

### 3.3.4 Developmental reductions in brain state variability are driven by stabilization of cognitive but not visuomotor processes

After observing that brain state variability overall decreased during development, we considered possibility that variability associated with the different brain state components might exhibit different developmental trajectories. For each session, we separately computed the proportion of BOLD signal variability associated with VME, maintenance, and retrieval brain state fluctuations by summing the contributions of their mean and spatial components. We then applied the same linear mixed-effects model outlined above to analyze the developmental trajectories of each component (Figure 11).

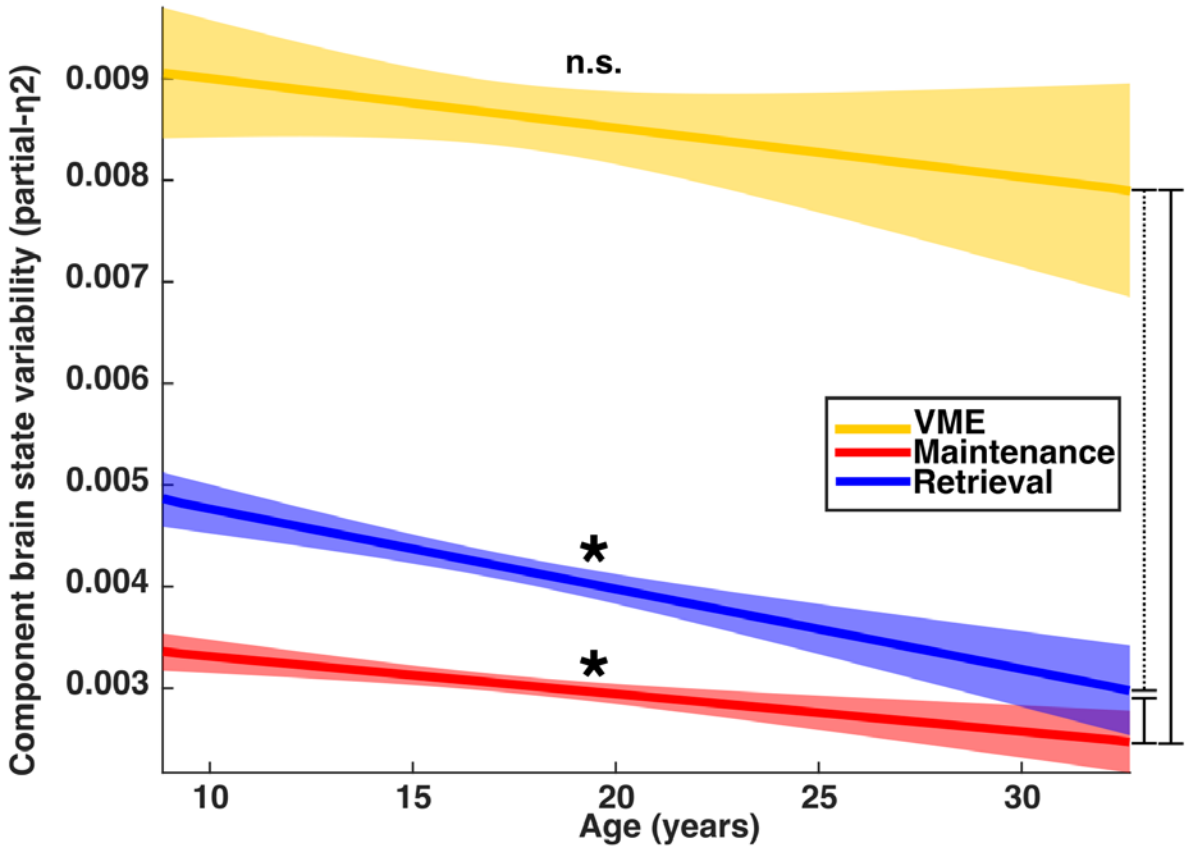


**Figure 11. Developmental changes in brain state variability**

**Depicts the developmental trajectories for VME (yellow), maintenance (red) and retrieval (blue) components of brain state variability. Single asterisks indicate significant individual slopes of brain state component variability; vertical lines connecting endpoints represent pairwise comparisons of slopes. Dashed and solid lines indicate a significant, and non-significant differences respectively.**

We found that whole-brain BOLD signal variability associated with trial-to-trial fluctuations in the VME brain state components did not significantly change across age at the group ($t(330)=-1.46$; $p=0.15$) or individual level ($t(330)=0.72$; $p=0.47$). Furthermore, we did not observe any relationship between VME brain state variability

and either of our measures of in-scanner movement ($t(330)=0.74$; $p=0.46$) or residual motion artifacts ($t(330)=0.47$; $p=0.64$). However, increased total VME brain state variability was associated with fewer correctly performed and valid trials ($t(330)=-3.66$; $p=0.0003$).

Total maintenance-related brain state variability decreased with age, an effect that was significant at both the group ($t(330)=-3.8$; $p=0.0002$) and individual level ($t(330)=-5.24$; $p=2.9e-7$)). Maintenance brain state variability exhibited no relationship with estimated in-scanner displacement ($t(330)=-1.3$; $p=0.19$)), but showed a trend toward a positive relationship with residual linear motion artifact that did not quite reach significance ($t(330)=1.86$; $p=0.063$)). The maintenance component of brain state variability was unrelated to differences in the number of correct and valid trials ($t(330)=-0.58$; $p=0.56$)).

Retrieval-related brain state variability, like the variability associated with the maintenance brain state components, also decreased with age, a change that was observable at both the group ($t(330)=-5.55$; $p=5.9e-8$)) and individual level ($t(330)=-2.84$; $p=0.005$)). None of the measures of in-scanner displacement, linear motion artifacts, or the number of correct and valid trials showed any significant relationship with retrieval-related brain state variability (all $p > 0.4$).

Next, we wanted to determine whether the developmental trajectories of brain state variability differed for VME, maintenance, and retrieval states. To do this, we performed pairwise comparisons of the slopes of the age-trajectories for each component using a mixed-effects model that was nearly identical to that used in the

preceding analyses, but which contained additional term to capture the interaction between group level age and brain state component

We found that the developmental trajectory of maintenance-related brain state variability was significantly shallower than both VME ($t(664)=2.64$; $p=0.008$) and retrieval-related ($t(664)=-4.12$; $p=4.26e-5$)) brain state variability. In contrast, our comparison of the trajectories of VME and retrieval-related variability did not reveal any significant difference between the slopes of their trajectories ($t(664)= 0.62$; $p=0.54$)).

### 3.3.5 Individual developmental trajectories of reaction time variability are predicted by changes in brain state variability

Our trial-to-trial analyses demonstrated the relationship between fluctuations in the amplitude of brain state expression and performance variability. Next, we sought to determine whether individual age-related changes in brain state variability could directly account for individual trajectories of behavioral variability. To address this, we leveraged the longitudinal design of our dataset to examine how individual differences in the developmental trajectories of reaction time variability and saccade precision were related to individual developmental trajectories of brain state variability.

We selected a subset of 29 subjects for whom we had at least four complete sessions of data. This amounted to 116 sessions of data acquired from a set of subject whose ages ranged from 12-30 years (mean=21 years; std=3.75). We computed total brain state variability per session as the proportion of BOLD signal variability uniquely attributable to brain state variability during the 0–5 TR range around each memory-

guided saccade that was determined in the previous analyses. We estimated regression weights for an inverse age factor that modeled the individual developmental trajectories of reaction time variability and precision, controlling for task condition and mean reaction time. We compared these individual trajectories of behavioral variability to trajectories of brain state variability and found that subjects who exhibited the greatest reduction in total brain state variability across sessions were also those who showed the greatest decreases in reaction time variability (r=-0.48; p=0.0084) (Figure 12**a**). The within-subject relationship between brain state variability and saccade precision however was not significant (r=0.28; p=0.13) (Figure 12**b**).

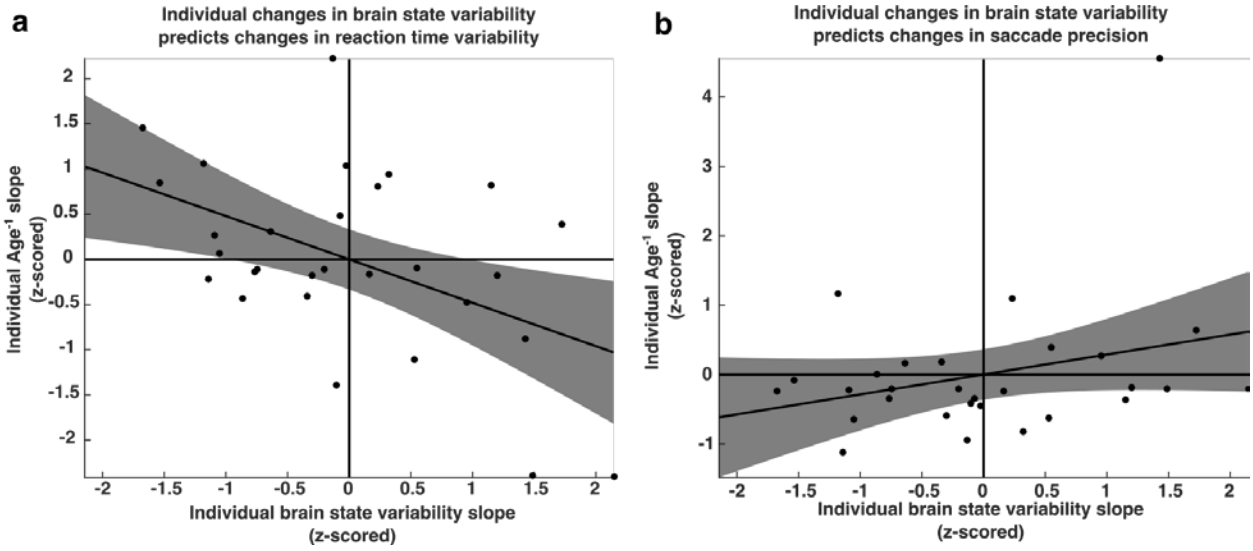


**Figure 12. Individual changes in behavioral and brain state variability**

**The relationship between changes in brain state variability and changes in a) reaction time variability and b) memory-guided saccade precision for a group subjects (n=29) for whom we had four of more complete sessions of data. The x-axes depict the slope of age-related change in brain state variability, computed separately for each subject. They y-axes depict the regression weight for the Age$^{-1}$ term used to fit each subjects'**

**behavioral data. Thus, a negative relationship indicates that greater reduction in brain state variability is associated with a greater reduction in behavioral variability.**

Due to the modest relationship between brain state variability and saccadic error at the single trial level, we considered the possibility that we might be underpowered to detect the within-subject longitudinal relationship between total brain state variability and saccadic precision in our smaller sample size. We expanded our analyses to investigate whether differences in brain state variability across sessions would predict deviations from the group-level average developmental trajectory of saccade precision. We therefore added brain state variability as a factor in a regression model using subject identity as random effect and including group and individual level age terms; task condition terms; and in-scanner motion estimates. We found that subjects who exhibited greater overall brain state variability tended to produce memory-guided saccades with reduced precision ($t(1332)=3.35$; $p=0.0008$).

## 3.4 DISCUSSION

Reduced behavioral variability is a key component of improvements that occur throughout adolescence on a wide variety of tasks. We demonstrated an example of this stabilization using a working memory task in which subject's performance of a memory guided saccade both improved on average and became more consistent with age. To understand the neural basis of developmentally stabilized behavior, we

investigated the relationship between variation in reaction time and accuracy of eye-movements and fluctuations of global neural gain signals that affect the amplitude of expression of whole-brain states of activity underlying distinct task-related processes. We found that while the average expression of these states was similar across subjects of all ages, variability in the expression of task-related brain states was associated with trial-to-trial variability in the reaction time and accuracy of memory-guided saccades. Importantly, this brain state variability represented fluctuations in the *amplitude* of brain state expression across trials, not simply variability in the *timing* of their expression or global fluctuations in mean activity (see Appendix C).

Additionally, variability in the expression of the mean and spatial components of the VME state, as well as the spatial component of the maintenance brain state, mirrored the higher-order phenomenon of the speed-accuracy trade-off. This finding is consistent with recent theoretical models [65] and empirical data from non-human primates [66] suggesting gain modulation plays a role in optimization processes that result in the speed/accuracy trade-off. We observed that trials with greater expression of working memory brain states were trials in which subjects tended to be faster and more accurate. We also observed that greater expression of the VME states occurred during trials that were both fast and less accurate. These findings can be related to our computational model of memory-guided saccade performance (detailed in the first chapter) by positing that increased VME gain reduces response thresholds, possibly via cortico-collicular inputs from pre-frontal and parietal regions [67], and that variability in working memory gain is accurately reflected by changes in maintenance state expression. On trials with low response thresholds (greater VME

expression), subjects tend to be faster, but more error prone. This is because less input to the oculomotor system is required to evoke an eye-movement —meaning that they can be fast— but they tend to be evoked more often by noise —meaning they are less accurate. Trials with high working memory gain (greater maintenance state expression) tend to be faster and less error prone because increased gain both speeds responses and increases the signal to noise ratio of the input to the oculomotor system, improving accuracy.

We hypothesized that developmental decreases in the variability of global gain signaling would result in stabilized expression of task-related brain states. Accordingly, we determined whether the expression of brain states associated with the working memory processes, visuomotor/encoding (VME), maintenance, and retrieval exhibited similar or different trajectories of variable expression across development. We found that the variability of the VME states did not decrease with age although they were significant predictors of single trial performance. Our task design did not allow us to dissociate the activity involved strictly in working memory encoding from that involved strictly in the visuomotor response, however, the re-expression of the mean VME state during the memory-guided saccade suggests that the state is largely dominated by visuomotor activity. In contrast, working memory maintenance and retrieval processes, whose fluctuations were also related to trial-wise performance, showed significant decreases in the variability of their expression. Perhaps most significantly, we found a strong relationship between individual longitudinal changes in total brain state variability and changes in reaction time variability as well as a relationship between average total brain state variability and average memory-guided saccade precision. Combined, our

findings provide compelling evidence that adolescent developmental changes in behavioral variability are driven by the stabilization of gain signals specifically affecting cognitive processes while gain signals affecting sensorimotor processes have largely stabilized prior to adolescence.

A complex interplay between top-down control [68], [69], and a mixture of contributions from several interconnected neuro-modulatory systems, each exerting its particular influence on ongoing sensorimotor, and cognitive processes [63], [70]-[72] may underlie these developmental changes in brain state variability. Recent fMRI studies have shown that fluctuations in the activity in midbrain and brain stem nuclei affect resting state connectivity in what appears to be a functionally organized way [73]. Similarly, cholinergic modulation has been shown to amplify the spatially selective effects of perceptual processing and attention in a manner analogous to fluctuations in our spatial brain state components [45], [63], [72]. Finally, myelination and synaptic pruning, which continue to progress in critical brain systems [13], [74], [75], occurring at different rates for different brain regions, may also affect neural signal to noise ratios and play a role in the stability of gain signals that contribute to behavioral variability. Differing rates of development in any of these systems could produce distinct developmental trajectories for the components of brain state variability.

The presence of brain state variability also bears upon the interpretation of brain/behavior correlations in general. In studies of single unit and population activity in non-human primates, correlations between the trial-to-trial fluctuations of neuronal activity and behavioral responses, often termed choice-probability (CP) or detect-probability (DP), have been interpreted as signifying a neuron's causal role in the

behavior [52]. It has been proposed, however, that brain-behavior relationships like CP and DP, might reflect a neuron's covariation with a neuronal gain signals, such as attention, rather than direct causal involvement [53], [76]. Brain state variability is consistent with this hypothesis and expands upon it in two ways 1) That brain state variability is the correlated fluctuation of many task-related (but not necessarily behaviorally relevant) brain regions suggests that brain behavior correlations like CP and DP should be wide-spread throughout task-related brain areas; and 2) Our finding of distinct developmental trajectories of brain state variability affecting different task-related processes suggests that fluctuations in multiple functionally specific global gain signals contribute to observed brain behavior correlations.

In light of the forgoing results and discussion, we propose that behavioral variability during working memory tasks is the result of variability affecting multiple global gain modulating signals, and the reduction in behavioral variability observed with development into adulthood is the result of the stabilization of gain modulating signals that affect primarily cognitive and not sensorimotor processes.

# 4.0 DEVELOPMENTAL DIFFERENCES IN BOLD SIGNAL DIMENSIONALITY

## 4.1 BACKGROUND

Neural complexity, an important aspect of neural variability, changes across the lifespan. Measures of variability and complexity are closely related: While variability quantifies the magnitude of a neural signal's instability around its mean, complexity metrics quantify the number of distinct ways in which that neural variability is expressed. EEG studies have shown that neural signal complexity during task performance increases during early childhood development [77] and from childhood through young adulthood [14], [15]. Studies of neural variability in later life have shown that BOLD signal variability begins to decrease [16], [78] and become less complex with age [79], [80], tracking decline in cognitive function. Thus evidence suggests that the complexity of neural activity follows an inverted U-shaped trajectory from childhood to late adulthood.

While it might be supposed that behavioral variability would increase as neural activity becomes more variable or complex, most studies that have examined the relationships directly have found the opposite to be true [14], [15], [78], [81]. The prevailing theory explaining these observations is that patterns of neural variability, even at rest, reflect the exploration of available neural states [82]. The mature brain, with its

regional balance of differentiation and specialization [83], allows for a greater degree of neural variability [84] by supporting a greater number of metastable states of activity and facilitating transitions between them [14]. Put simply: as you mature, it is supposed more patterns of neural activity are accessible and it's easier to get from one pattern to another.

In our experiments we have observed that behavioral performance and neuronal dynamics continue to change across development: that reaction times and accuracies both improve and stabilize, seemingly in tandem with an age-related decrease in BOLD signal variability associated with brain-wide gain signals. On its face, it would appear that our results stand in contrast to the aforementioned experiments showing developmental decreases in behavioral variability being associated with increases in neural variability and complexity. To reconcile this seeming discrepancy, we set out to determine 1) whether the developmental trajectories of brain state variability are distinct from the trajectory of neural complexity and 2) whether after accounting for age-related differences in brain state variability age-related changes in neural complexity still predict developmental changes in behavioral variability.

## 4.2 METHODS

We used the longitudinal behavioral and fMRI data set detailed in the first two chapters of this dissertation. For our analyses of behavioral variability, we examined reaction time variability and the precision of memory-guided saccades. Reaction time variability was

defined as the standard deviation of reaction time for each type of trial within a session. Precision was defined as the standard deviation of the distribution of memory-guide saccade endpoints around their mean for each target during each task condition.

Because we were interested in estimating the complexity of the neural activity that was not consistently associated with task events or global gain modulation, we analyzed volumes of fMRI data that had both the average task responses as well as brain state fluctuations removed from them (see Appendix). Briefly, we removed the average task responses along with motion and other nuisance covariates from the fMRI time series, using finite impulse response regression that does not assume a shape for the hemodynamic response function. Subsequently, we removed residual variability due to trial-to-trial fluctuations in task-related brain state expression by regressing the set of canonical brain state patterns from each volume of task data. This process produced a set of doubly residualized whole-brain time series from which variability related to average task responses, brain state fluctuations, and other nuisance artifacts have been removed.

As a measure of neural complexity, we estimated the intrinsic dimensionality of the doubly residualized BOLD time series in two ways: 1) by performing dimensionality reduction using principle components analysis (PCA) [85] and selecting the number of components that explained 50% of the remaining BOLD signal variability for each session; and 2) by estimating dimensionality using a maximum-likelihood estimation (MLE) based procedure [86].

We used linear mixed-effects models with a unique subject identifier as a random effect parameter to account for the longitudinal nature of the data set and differing

numbers of session across subjects. In all of our analyses, unless otherwise noted, we controlled for differences in motion between sessions by including measures of average frame-wise displacement, a measure of residual motion artifacts (see Appendix), the percentage of BOLD signal variability associated with brain state variability, and the percentage of identifiably correct trials as nuisance regressors.

## 4.3 RESULTS

### 4.3.1 The dimensionality of BOLD signal residuals increases with age

We computed two metrics of BOLD signal complexity, principle component (PC) dimensionality, and maximum-likelihood estimated (MLE) dimensionality, and found that both methods produced qualitatively similar estimates (Figure 13)**.** To quantify their similarity, we regressed the estimates of PC dimensionality on MLE dimensionality and found their relationship to be highly significant (t(326)=19.833; p=5.59e-58).

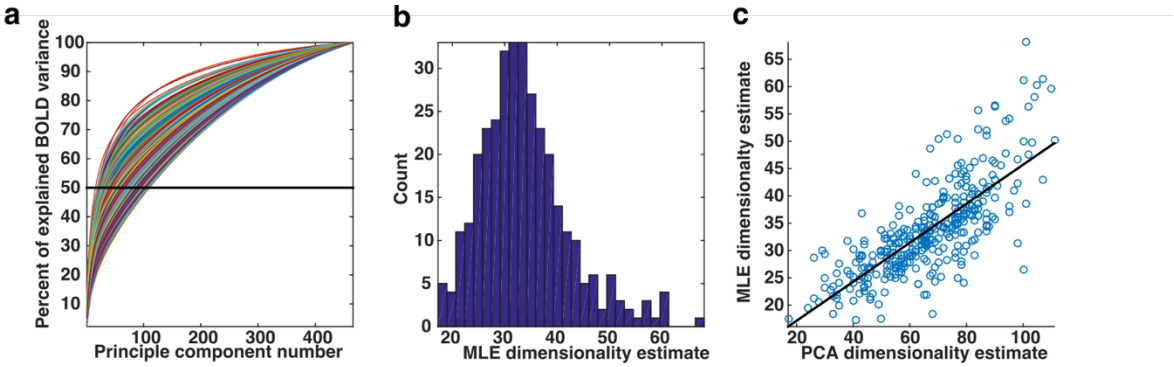


**Figure 13.** Comparing methods for estimating BOLD signal dimensionality

**a) Cumulative percentage of whole-brain BOLD signal variance explained across principle components. Each colored curve represents one session. One measure of neural complexity is based on the number of principle components required to explain 50% of BOLD signal variability (black horizontal line). b) Histogram depicting the distribution of dimensionality estimated derived using a maximum-likelihood procedure. c) Scatter plot depicting the high degree of agreement between the two estimates of dimensionality.**

Next we explored the relationships between residual BOLD signal complexity and age while controlling for potential confounding factors. Our earlier work has shown that younger subjects exhibited greater brain state variability and more residual motion-related artifacts. After removing these sources of BOLD signal variability, the residual data for younger subjects may have artificially exhibited lower dimensionality. In addition, session-to-session differences in the percentage of correctly performed trials could influence the estimates of the hemodynamic response function and thereby affect the dimensionality of the residuals.

We found that greater average frame-wise displacement and residual motion artifact estimates were significantly associated with reduced BOLD signal complexity estimated using the PC method (displacement: $t(330)=-8.9$; $p=4.12e-17$; motion resid. est.: $t(330)=-16.25$; $p=4.6e-44$). However, the MLE-based metric only exhibited a significant negative relationship with the residual motion artifact measure ($t(330)=-9.97$; $p=1.24e-20$) and not per-frame displacement ($t(330)=-1.18$; $p=0.24$). Similarly, greater brain state variability during a session was also associated with reduced PC

dimensionality (t(330))=-5.86; p=1.01e-8) and MLE dimensionality (t(330))= 3.35;p=0.001). Neither, PC nor MLE dimensionality exhibited a significant relationship with the percentage of correctly performed trials (p=0.47; and p=0.46 respectively).

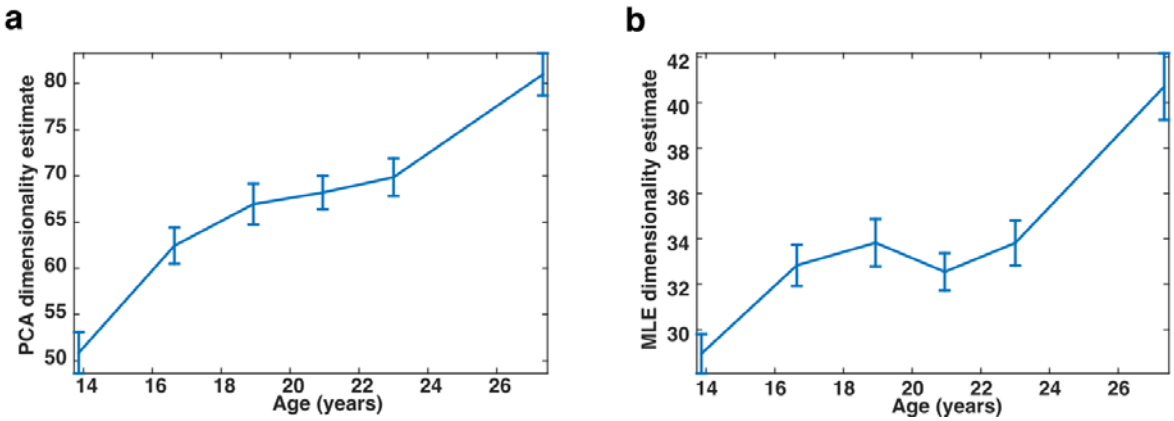


**Figure 14. BOLD signal complexity increases with age**

**a) Estimate of BOLD signal complexity using the number of principle components required to account for 50% of the whole-brain BOLD signal variance. b) BOLD signal complexity as estimated using a separate maximum-likelihood based procedure. X-axes depict the age of the subject and y-axes indicate the respective dimensionality estimates. The data was adaptively binned so that each point contains equal number of data samples. Error bars represent one standard error of the mean.**

Nevertheless, as Figure 14**a-b** shows, after controlling for potential confounding factors, both estimates of BOLD signal complexity increase with age (PCA: t(330)=5.93, p=7.66e-9; MLE: t(330)=3.20; p=0.0015), consistent with prior literature. In addition, age remained a significant predictor of PC and MLE dimensionality after the addition of quadratic terms for brain state variability and in-scanner motion as well (data not shown).

### 4.3.2 Dissociable relationships between behavioral variability, brain state variability and BOLD signal complexity

Next, we separately examined the relationship between behavioral variability and both measures of BOLD signal complexity while controlling for brain state variability and motion-related factors. For this analysis we omitted age-related covariates to assess these relationships while retaining variance associated with development. We found that reaction time variability decreased as PC dimensionality increased ($t(1337)=-2.8137$; $p=0.005$), but did not observe a significant relationship with MLE dimensionality ($t(1337)=-1.26$; $p=0.21$). Improved saccade precision was also associated with greater BOLD signal complexity assessed using PC estimation ($t(1337)=-3.12$; $p=0.07$) and MLE ($t(1337)=-2.07$; $p=0.04$)). Importantly, for each model, increased brain state variability remained a significant predictor of greater reaction time variability and reduced saccade precision.

It is possible that the relationship between increasing neural complexity and stabilizing behavioral performance is correlative, that neural activity does become more complex with age, but that this occurs in parallel with the development of other processes responsible for stabilizing behavior. Stronger evidence for a potential causal link would be the presence of a significant relationship between behavioral variability and BOLD signal complexity after known age-related changes are accounted for. We therefore re-examined these relationships, this time including $Age_{first}^{-1}$ and $Age_{relative}^{-1}$ (see Chapter 1 methods) terms as well as their interactions with task condition.

Because of the inconsistent relationship between behavior and MLE dimensionality, we limited this analysis to the PC estimates of BOLD signal complexity.

We found that after accounting for age in our regression models, the relationship between BOLD signal complexity and reaction time variability was no longer significant ($t(1331)=-1.07$; $p=0.29$) while a significant positive association with brain state variability remained ($t(1331)=1.96$; $p=0.05$). In contrast, saccade precision maintained the direction and significance of its associations with BOLD signal complexity ($t(1331)=-2.45$; $p=0.014$) and brain state variability ($t(1331)=2.51$; $p=0.012$). This finding indicates that differences between subjects and sessions in the variability of memory-guided saccade end points —differences that are not simply the result of average age-related improvements in precision across adolescent development— are independently and differentially related to differences in in the complexity of neural activity during the task as well as well as brain state variability.

## 4.4 DISCUSSION

Neural variability has been proposed as an index of age and cognitive function [87]. Support for this idea has come from experiments examining a wide range of ages consistently finding that increases neural variability and complexity, at rest and during task, are associated with more stable behavioral performance [14], [15], [79], [80]. The mechanisms underlying this association are unknown, but it is hypothesized that increases in the complexity of resting state activity may be due to the exploration of a

greater range of possible activity states that become available during peak cognitive development [82]. In a similar vein, it has been proposed that the ability to quickly transitions between states of neural activity develops in concert with the ability support more states of activity during task performance, resulting in trial-to-trial inconsistencies in the patterns of neural activity and increased estimates of neural complexity [14].

Here, we considered a possible alternative to this last view: that the increase in signal complexity that attends stable behavior performance reflects the ability of the maturing brain to successfully support task states alongside (or in superposition with) an increasing number of task-irrelevant states. According to this hypothesis, the increase in signal complexity during task performance does not reflect the presence of additional behaviorally equivalent metastable task states, but the concurrent exploration of task-irrelevant states that minimally affect task-related activity. The absence of age-related differences in the mean amplitude of expression of task-related brain states (see Chapter 2) suggests that the additional states of neural activity observed in older subjects during task performance do not interfere with the expression of task-related activity, consistent with this hypothesis.

The observed correlation between developmental changes in behavioral variability and neural complexity is also consistent with this hypothesis. However, rather than indicating a causal role in stabilizing behavior, the correlation would simply reflect that the development of the ability to support non-task states occurs in parallel with the development of other processes —such as stabilizing gain signals— that actually stabilize performance.

In this study, we tested this hypothesis by measuring developmental changes in relative BOLD signal complexity after removing mean task responses and whole-brain variability associated with fluctuations in global gain signals. We used two different methods, to estimate BOLD signal dimensionality, a proxy for signal complexity, one based on principle component decompositions, and the other based on maximum-likelihood estimation. Both measures produced quantitatively similar estimates of BOLD signal complexity, demonstrating that a developmental change in BOLD signal complexity is unlikely to be an artifact of dimensionality estimating procedures.

Consistent with prior literature, we observed a significant age-related reduction in both estimates BOLD signal complexity. Importantly, we observed that both reaction time variability and memory-guided saccade precision exhibited distinct opposing relationships with brain state variability, a putative measure of whole-brain gain stability and neural complexity when both terms are included in the regression model. This finding suggests that brain state variability and neural complexity represent distinct factors associated with stabilizing behavioral performance.

Stronger evidence (but still by no means definitive) for neural complexity playing a causal in stabilizing behavioral would be if it was correlated with the individual differences in behavioral variability after accounting for the average effects of age-related behavioral stabilization. Our results on this front were mixed: we found that after accounting for age and session-to-session differences in brain state variability neural complexity was not significantly associated with reaction time variability. However, saccade precision was improved in subjects with greater BOLD signal complexity.

In sum, our results suggest that developmental improvements in reaction time variability during the memory-guided saccade task are primarily driven by the stabilization of gain signals. However, developmental improvements in saccade precision are only partly accounted for by stabilizing gain signals. The remaining relationship between increasing neural complexity and improving saccade precision may reflect that the fidelity of working memory representations are improved by having access to a greater set of states of neural activity —akin to the proposal by McIntosh and colleagues [14]. Alternatively, working memory fidelity may be improved by other processes, such as improving signal to noise ratio through continued myelination and synaptic pruning [74], [88], [89], which are distinct from gain stability and neural complexity, but develop in tandem with them.

# 5.0 SUMMARY AND DISCUSSION

Compared to other cognitive processes, working memory exhibits a prolonged time course of maturation [5], [6], [8]. The experiments and analyses outlined in this dissertation were designed to explore how developmental changes that occur during adolescence affect the neural mechanisms supporting working memory.

In contrast with the majority of developmental studies, we focused mainly on changes in behavioral variability, the trial-to-trial fluctuations in reaction time and accuracy, as an index of developmental improvement in working memory performance. Our motivation, in part, stemmed from evidence suggesting that behavioral variability is an important index of cognitive functioning in non-developmental contexts; Instabilities in behavior are associated with cognitive decline in normative aging as well as impairments due to psychiatric disorders, like ADHD, schizophrenia, depression and borderline personality disorder [10], [30]. Bolstered by recent evidence that behavior also stabilizes during adolescence [13], [14], we reasoned that the sensitivity of behavioral variability as a measure of cognitive function would make also make it a sensitive measure of adolescent working memory development.

We found that the variability of reaction times and the precision of memory-guided saccades improved during adolescence and exhibited similar developmental

trajectories to their mean counterparts. This tendency for behavioral performance to stabilize as well as improve on average more or less in parallel suggests that developmental changes affecting a common set of neural mechanisms are responsible for both facets of developmental improvement.

The idea that improvements in mean behavior and behavioral variability might be supported by a common mechanism received support from our computational analysis of memory-guided saccade performance. We initially began our simulation studies in an effort to account for an unexpected, and seemingly age-invariant, U-shaped relationship between reaction time and the magnitude of saccadic error. We expanded on the drift diffusion modeling framework to simulate hypothesized working memory retrieval processes involved in the memory-guided saccade task. Our results indicated that the speed-accuracy relationship that we observed could be accounted for by a balance of independent variability affecting the gain of working memory representations and the response thresholds of oculomotor related neurons.

More interesting, however, was our finding that coordinated developmental reductions in the variability of working memory gain and response thresholds could account for improvements in behavioral variability *and* mean behavior, while minimizing (but not completely eliminating) age-related changes in the speed-accuracy tradeoff. That is, by stabilizing gain and response thresholds, and leaving their mean values unchanged, the reaction times of simulated saccades became faster and less variable while at the same time becoming more accurate. Developmental stabilization of gain and response thresholds may therefore be a mechanism by which behavior improves and stabilizes in parallel during development.

Importantly, the correlation between behavioral performance and behavioral variability was not total; That a prediction of subject age from behavioral performance was significantly improved by including reaction time variability as an additional factor, indicates that developmental changes that promote trial-to-trial stability in reaction time are somewhat distinct from those that support speeding reaction time on average. This finding suggests that developmental changes in behavioral performance are not likely to be completely accounted for by mechanisms, like that described by our diffusion model, that tightly yoke mean behavior and behavioral variability.

Understanding the mechanisms underlying developmental changes in behavioral variability has only somewhat recently become an active area of research. Analyses of structural and electrophysiological data have revealed that changes in behavioral variability are correlated with the development of white-matter tracts and the complexity of neural activity [13], [14]. While a full mechanistic understanding of how either of these phenomena relate to behavioral variability is lacking, one proposed hypothesis is that the development of structural connectivity allows for a greater repertoire of possible states of neural activity. The ability to support multiple states allows neural activity to become more complex partly by enabling additional metastable states of activity. Proponents of this view, operating from an analogy with the phenomenon of stochastic resonance [90], have also proposed that a certain amount of noise or variability might play a causal role in stabilizing behavior by facilitating neural computations [14], [91].

Behavioral variability in a non-developmental context has been addressed more fully by electrophysiologists working with non-human primates. Two important contributions from theoretical and empirical experiments have been the recognition that

in order for correlations between neural activity and behavior to be observable, interneuronal correlations must be present [52], [53], and that fluctuations in neuronal gain signals, possibly due to top-down attention, contribute significantly to the presence of these interneuronal correlations [61], [92].

In Chapters two and three of this dissertation, we explored the contributions of gain modulation and neural complexity to developmental changes in behavioral variability. We found that putative trial-to-trial fluctuations in gain modulation, which manifest as changes in the amplitude of expression of whole-brain task-related states of activity, were associated with reaction time and accuracy. Most significantly the decreases that we observed in the magnitude of whole-brain gain modulation (or brain state variability) predicted individual changes in reaction time variability. These results support the hypothesis that the stabilization of behavior during adolescence is related to the stabilization of global gain signals. Moreover, our computational analyses of memory-guided saccade performance indicate that, at least in principle, a developmental reduction in gain variability can account for developmental changes in mean behavioral performance as well.

We also found that when developmental trajectories of brain state variability were decomposed into visuomotor, maintenance, and retrieval related components, distinct trajectories emerged. To make sense of this result, we proposed that multiple functionally specific mechanisms supporting global gain modulation might exist and mature at different rates. As a potential avenue of future research this is particularly appealing.

Evidence for a role for neural complexity in behavioral variability remains mixed. We were able to replicate other researchers observations of increasing neural complexity with age, as well as the negative relationship with behavior variability. However, after controlling differences in age and brain state variability, neural complexity only remained significantly associated with saccade precision.

As described above, there are two hypotheses regarding neural complexity: 1) that it reflects the presence of addition states of activity that emerge with age; in which case its relationship with behavioral variability is largely an epiphenomenon; or 2) that the neural complexity, as measured by EEG and fMRI, reflects the presence of a kind of noise which facilitates neural processing. The mediating effect of age and brain state variability on the relationship between reaction time variability and fMRI dimensionality supports the former view. The remaining significant relationship between BOLD signal complexity and saccade precision, however, means that we cannot completely discount the hypothesis that increased neural complexity is causally involved in improving the precision of memory-guided saccades.

Taken together, our experiments add support for a model of continued development of working memory processes during adolescence. Results from our empirical and computational analyses expand on the current body of developmental research by providing evidence that a significant mechanism underlying developmental improvements in mean behavioral performance and behavioral variability is the stabilization of global gain signals.

# APPENDIX A

## EYE-MOVEMENTS

Eye-movements were recorded in the scanner with an infrared camera system equipped with long-range optics and sampling at 60Hz (Model R-LRO6, Applied Science Laboratories, Bedford MA). Subject’s compliance with instructions was assessed and eye-movements were monitored via remote video during task performance. We used a nine-point calibration procedure to estimate the transformation from the eye-tracker's native encoding space to on-screen pixel location. Saccadic events were detected using an in-house suite of automation routines. Individual saccade candidate events were detected from local maxima in the eye-movement velocity trace. Saccade start and end times were determined by searching backward and forward in time in the velocity trace to find the sample where velocity dropped below 1/10th of the peak velocity.

.

# APPENDIX B

## DRIFT DIFFUSION MODEL OF MEMORY-GUIDED SACCADE PERFORMANCE

We employed a simple multi-dimensional extension of the drift diffusion modeling framework to simulate the reaction time and accuracy of memory-guided saccades. In this model, the activity of a group of motor-response related neurons, during trial $\boldsymbol{m}$ is represented by a vector $\boldsymbol{S(m, x, t)}$**,** which begins at zero and evolves over time, $\boldsymbol{t}$, until one of the vector entries, $\boldsymbol{x}$, exceeds a threshold value $\boldsymbol{V(m)}$. Each entry in $\boldsymbol{S}$ indexed by $\boldsymbol{x}$ represents a neuron whose activity, once it exceeds $\boldsymbol{V(m)}$, will result in a saccade being performed to location $\boldsymbol{x}$**.**

For each trial $\boldsymbol{S}$ evolves over time, $\boldsymbol{t}$, in the following way:

$\mathbf{S(m, x, t)} = \mathbf{S(m, x, t-1)} + \mathbf{M(m, x, t)} + \mathbf{A(m)} * \boldsymbol{\mu}\mathbf{(x)} + \boldsymbol{\varepsilon}\mathbf{(\sigma, m, x, t)}$ , subject to $\boldsymbol{V(m)}$

**Equation 7. High dimensional drift diffusion model**

Where:

I. $\boldsymbol{\mu(x)} = \boldsymbol{exp}(-(\boldsymbol{x} - \boldsymbol{x_0})\mathbf{2} \,/\, \boldsymbol{\tau})$ and $\boldsymbol{x_0}$ represents the location of the remembered target and $\boldsymbol{\tau}$ the width of the point spread function linking the working memory representation to the motor representation.

II. $\boldsymbol{A}(\boldsymbol{m})$ represents the trial-to-trial modulation in working memory gain. When this value is high, $S$ accumulates the working memory representation more quickly.

III. $\boldsymbol{\varepsilon}(\boldsymbol{\sigma}, \boldsymbol{m}, \boldsymbol{x}, \boldsymbol{t})$ represents spatially and temporally independent Gaussian noise, with a standard deviation given by $\boldsymbol{\sigma}$, which accumulates over time into $\boldsymbol{S}$.

IV. $\boldsymbol{A}(\boldsymbol{m})$ and $\boldsymbol{V}(\boldsymbol{m})$ were drawn from uniform distributions centered on a mean value. The ranges of these distributions were selected so that gain and threshold were never negative.

For simulations exploring changes in gain variability and response threshold variability, e $\boldsymbol{\sigma}$ was held fixed at $4.5$; $0 \leq \boldsymbol{x} \leq 5$; $\boldsymbol{\tau} = 0.7$; $\boldsymbol{S}(\boldsymbol{m})$ was as 50x1 vector.

# APPENDIX C

# FMRI PROCESSING

## C.1 ANATOMICAL PREPROCESSING

T1-weighted anatomical images were reconstructed from raw DICOM files and converted to NIFTI format. We estimated the bias field corrections using smoothed and highness filtered anatomical data analyzed with FSLs *fast* algorithm. After bias field correction we constructed a skull stripped anatomical data set for the subject, which we used to estimate the 12 degree-of-freedom affine transformations that would align the subjects data with the MNI152 anatomical template. Lastly we computed the non-linear transformation that would bring the subject's affine-aligned anatomical data set into registration with the MNI152 template. We saved final combined linear/-non-linear transformation for later use in registering the subjects' functional data to the standard space.

## C.2 FUNCTIONAL PREPROCESSING

fMRI data were preprocessed using a combination of AFNI and FSL software. In our pre-processing pipeline, raw data was converted from DICOM format to NIFTI volumes and slice-timing correction was applied using AFNI tools. We performed motion estimation and correction in two phases. First we pre-aligned each frame of a subject's functional data to a volume created by taking the temporal mean of the 4-D functional time series. Then, a second, "true", average functional volume was computed from the pre-aligned functional data, producing a reference functional volume that was less affected by motion artifacts. We then aligned each frame of the original function time series to this second reference volume using sinc-function interpolation and estimating the time course of translational and rotational motion throughout the run. We used these estimated time series throughout our later analyses of the functional data.

Next, using FSL's brain extraction tool, we stripped the skull and superfluous tissues from the subject's motion corrected mean functional EPI images, afterward aligning the resulting mean EPI volumes to their anatomical MPRAGE volume using a six degree-of-freedom rigid-body transformation estimated using spline interpolation. To align each frame of the motion corrected EPI sequence to the subjects structural image, we applied the translation estimated in the previous step to each frame of the motion corrected functional time series and then removed the skull and extraneous tissues from each frame of the functional time series. Tissue remaining within the mean functional volume after the skull stripping procedure was removed by applying a dilated binary mask to the mean aligned functional volume that removed extreme voxels whose values

did not reside in middle 98$^{th}$ percentile. We then removed voxel-wise temporal extrema using AFNI's 3dDespike software.

To align a subjects functional data to a standard MNI152 (Montreal Neurological Institute; MNI) template in a single transformation step, we used FSL *convertwarp*, and *applywarp* functions to combine the estimated motion correction, functional-to-structural, and linear and non-linear subject-to-MNI152 transformations into a single operator, which we applied separately to each frame of the original slice time-corrected functional data.

We performed minimal spatial smoothing on the aligned functional data, using a SUSAN algorithm with a 5mm FWHM kernel, followed by a conservative high-pass filtering of the voxel-wise time series, which removed or attenuated BOLD signal frequencies below 0.0083Hz (corresponding to fewer than 3 cycles per task run). Finally, we rescaled all voxel values by a value defined to be 10,000 divided by the global median.

# APPENDIX D

# FMRI ANALYSIS

## D.1 DECONVOLUTION

From each session's data we extracted eight voxel-wise average time courses of BOLD activity associated with each of the four task conditions for stimulus presentations in each visual hemifield. We estimated these time courses with a finite impulse response (FIR) regression model. FIR design matrices were constructed manually and applied to the voxel-wise time series using 3dDeconvolve (AFNI). All trials, including incorrect responses and blinks, for each stimulus type were modeled over an interval consisting of the duration (from initial stimulus presentation to the execution of the memory-guided saccade) plus an additional 22.5 seconds (15 TRs). The design matrix included nuisance regressors to account for the effects of signal drift, subject motion, and global signal changes as captured by white matter and cerebrospinal fluid (CSF) signals and their derivatives. Signal drift was modeled as a 3$^{rd}$ order Legendre polynomial time series.

Head motion was computed along six affine components corresponding to translation in the three cardinal directions and rotations about three orthogonal axes. In addition we computed a time course of total displacement for each session based on the Euclidean norm of the time derivative of the movement time series at each time point. To account for the prolonged effect of autocorrelated movement on the BOLD signal, we included temporally leading (-1TR) and lagging (+1-2TRs) copies of each of the seven motion regressors. Each of the seven motion time courses therefore contributed four motion regressors to the deconvolution design matrix. After deconvolution, we scaled the resulting whole-brain average trial time courses at each voxel, normalizing them to the standard deviation of the regression residuals at the same voxel location.

## D.2 IDEALIZED TIME COURSE

Idealized voxel-wise trial time courses for the long DI (9 second delay) conditions were estimated from the scaled average trial time course estimates. We modeled these separately for each condition and target hemifield using 3dLME (AFNI), a linear mixed-effects framework. Each time point was modeled as a separate categorical fixed effect and we did not include an intercept term in the model. To account for any bias due to the over representation of subjects who participated in more scans, we included subject identity as a random effect component in the regression model. For each trial type we computed the total Euclidean displacement undergone by each subject's brain during

the BOLD signal measurement intervals (trial durations plus 15 TRs) and included it as a fixed-effect component in the regression analysis. We calculated subjects' average age for all of their sessions and, after centering by the global mean, included it as a subject level fixed-effects regressor. We included a mean age by time interaction term to capture age-related differences in the voxel-wise time courses. We included the subjects' age at each session, after subject level mean-centering, as a second age-related random-effects regressor. Within a given voxel, a single whole trial time course may include independent contributions from visually- and memory-guided saccade events. To account for potential differences due to variability in the number of correct saccades, we included the proportion of unclassifiable and incorrect visually- and memory-guided saccades and their interactions with time as fixed-effect components of the model. We produced idealized trial time courses by generating the voxel-wise model estimates for a subject of mean age, mean in-scanner displacement, and perfect trial performance. This process generated four idealized whole-brain time series corresponding to both long-delay conditions in which targets were located in either the left or right visual hemifield. We used these idealized BOLD time series in our construction of the canonical brain states

## D.3 AVERAGE TIME COURSES OF BRAIN STATE EXPRESSION AND BRAIN STATE VARIABILITY

We converted the average whole-brain trial time series and whole-brain residual time series into average time courses of brain state expression and variability respectively. For each TR, we extracted the whole-brain pattern of activity that we then vectorized and modeled using a linear regression. Our design matrix consisted of vectorized versions of the six brain states (the mean and spatial components of the VME, maintenance and retrieval states) as well as the 19 nuisance regressors templates described above. For each TR we extracted the regression weights for the six brain states, motion, and nuisance components and ordered them into a time series. When performed on the whole-brain **average trial time series**, the result is a time course of expression of each of the brain states during a trial. When performed on the whole-brain **residual time series**, the result is a time course of brain state fluctuations, where positive values indicate that a particular brain state was present to a greater extent than average and negative values indicate that a state was expressed less than average. For each session, we converted the time course of brain state variability derived from the whole-brain residual time series into z-scores.

## D.4 TRIAL-TO-TRIAL BRAIN STATE AND BEHAVIOR RELATIONSHIP

For each session we separately transformed reaction time and saccadic error from each of the four main task conditions into z-scores. SE was rectified such that high SE values reflect greater error in memory-guided saccadic endpoints on a trial. We excluded all trials for which measurements of reaction time and endpoints for both visually- and memory-guided saccades were unavailable due to blink artifacts, noisy data, or transient loss of pupil- or corneal reflection-lock.

We related trial-to-trial variability in reaction time and accuracy to variability in the expression of each brain state across a range of times (±15 TRs) relative to the TR containing the subject's execution of a memory-guided saccade for each trial. Using all correct trials across all sessions, we extracted our z-scored measurements of brain state fluctuation derived from the whole-brain residual time series. We then constructed a regression model that included terms for the measured values of each brain state at the relative TR. We also included terms for the spatial brain state interaction with target hemifield. Each model contained terms that varied across trials but did not vary across relative TRs. These included terms for run number, target hemifield, target location (eccentricity), and the square of target location term. For the trial-to-trial reaction time model, we included a term for trial-to-trial SE and its square, and vice versa. This last set of regressor terms served as a null model against which the full brain state model was compared. The trial-wise reaction time and accuracy models were fit using a linear mixed-effects framework (MATLAB) to account for the different numbers repeated measurements for many of the subjects. Subject identity was modeled as a random

effect. We used the difference between the ordinary $R^2$ values for full and null models at each relative TR to assess the amount of unique behavioral variability accounted for by trial-to-trial fluctuations in the expression of different brain states. At each relative TR we compared the null and full modes using simulated maximum-likelihood estimation procedure with 5000 iterations (MATLAB).

## D.5 ESTIMATING BRAIN STATE VARIABILITY

For each session, we extracted a set of volumes from the normalized post-deconvolution residual time series that occurred within a window from 0–5 TRs relative to the memory-guided saccade. We applied the brain state, motion and nuisance linear regression model described above to each of the selected volumes. At each volume, we multiplied the regressors by their best-fit coefficients across voxels within the gray matter mask. We then computed the sum of squares for each set of brain state voxels within each regressor separately, as well as the sum of squares of the regression residuals within the brain state mask. This yielded an estimate of the total BOLD signal sum of squares error present across all grey matter that was attributable to brain state variability, motion and other nuisances, as well as unclassified variability. We computed these values for each of the selected volumes of residual data and added the resulting sums of squared error values separately for each regressor. Measures of total brain state variability and component brain state variability were calculated in a manner analogous to partial-$\eta^2$: total brain state variability was defined as the combined sum of

all brain state components (mean and spatial for each state) sum of squares, divided by the combined sum of all brain state component sums of squares as well as the unclassified sum of squares. Component variability was calculated similarly, except the numerator represented the sum of squared for a particular brain state component, e.g. mean and spatial VME or mean and spatial maintenance, rather than the total of all component sums of squares.

## D.6 WHOLE BRAIN MOTION REGRESSORS

We developed a method for estimating and removing temporally prolonged motion artifacts from fMRI data based on motion template volumes that model the spatial pattern of artifacts associated with the linear effects of motion. The initial deconvolution step for individual session data produced a regression coefficient for each temporally lagged motion regressor for each voxel. We normalized the voxel values within these volumes by the standard deviation of their post-deconvolution residuals and computed the mean patterns across all subjects. We used these whole-brain patterns of normalized regression coefficients to construct motion artifact templates. For each of the 28 templates (7 motion components with 4 temporal lags), we subtracted the spatial mean of all voxel values and scaled the resulting volumes to a common vector magnitude. Using principle component decomposition on the vectorized motion templates, we found a set of 11 motion templates that captured >90% of the variability in the set, which were then converted back into 3D volumes Error! Reference source not

found. In addition, we constructed a set of spatial gradient templates. We first created 3 spatial gradient volumes whose voxel values were equal to their x, y, and z coordinates relative to the volume's center of mass. We set each voxel that fell outside of a whole-brain MNI mask to zero. We then computed a set of 3 "interaction" templates that corresponded to each pair-wise product of the spatial gradient templates. Lastly, we constructed 2 constant offset templates. The first consisted of a whole-brain binary MNI mask. The second was the brain state mask. As a whole, this set of 19 templates constituted the set of spatial nuisance regressors that we used to capture and remove remaining unwanted spatial modes of whole-brain BOLD signal variability.

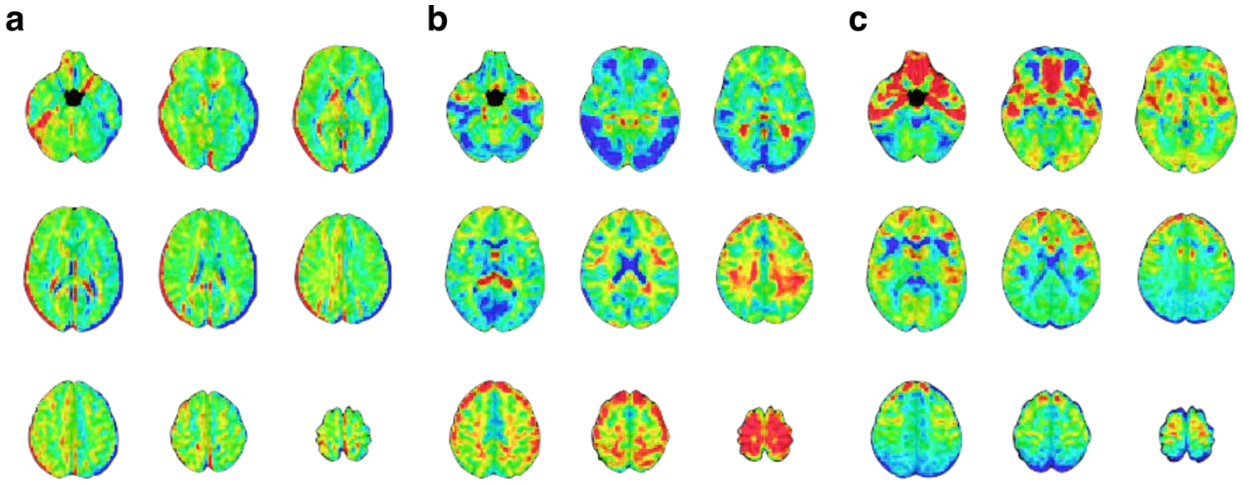


**Figure 15. Whole-brain motion regressors**

**Illustrative examples of three (a-c) whole-brain motion templates out of a total set of 19. We used this set of templates to account for motion related variability that remained in each TR of the whole-brain residual time series.**

## D.7 REACTION TIME SIMULATIONS

We observed that the direction of the trial-to-trial relationship between brain state expression and reaction time reversed (the transition from blue to red in some rows of the lower panel of Figure 10**a**). This inversion could result from a trivial trial-to-trial relationship between reaction time and the *timing*, not amplitude of brain state expression. We therefore performed three simulations of possible mechanisms that could give rise to a trial-to-trial relationship between the mean VME brain state and reaction time (Figure 10)

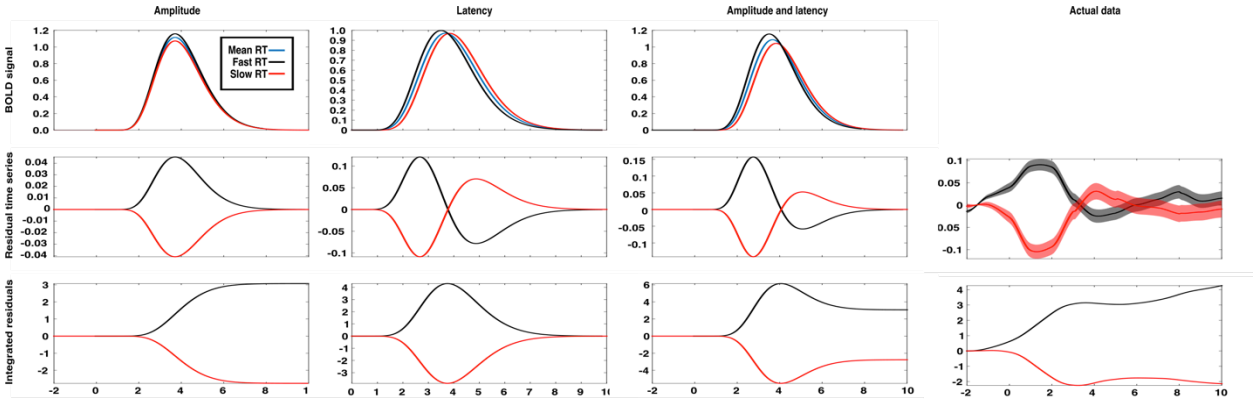


**Figure 16. A comparison of timing and amplitude effects on brain state expression**

**The x-axis of each panel represents time (in 1.5s TRs) relative to the execution of the memory-guided saccade. An amplitude relationship (1st column), a latency relationship (2nd column), and a combined amplitude and latency relationship (3rd column), are compared to actual data (4th column). The first row depicts the patterns of trial-to-trial BOLD signal variability for each mechanism. Trials are divided into fast (black) and slow reaction time (red) sets defined by a median split. The average BOLD signal across all trials depicted in blue. The average residuals time series (2nd row) for fast and slow trials exhibit distinct patterns for each possible mechanism. The time integral of the average**

**residuals makes this difference explicit: If a trial-to-trial relationship between the VME brain state and reaction time simply reflected trial-to-trial variability in the latency of the eye-movement and eye-movement evoked visual activity, then the integrals of the residual time series for fast and slow reaction time trials should both converge to zero (2nd column). However, the absence of this convergence in the mean VME brain state data (4th column) is consistent with either an amplitude-based relationship or a mix of amplitude and latency.**

A purely latency based explanation of the mean VME brain state/reaction time relationship predicts that the integral of the mean VME brain state residual time series, for both fast and slow reaction time trials should converge to zero (Figure 16**,** column 1). A relationship between reaction time and brain state expression mediated by fluctuations in the amplitude of expression of the brain state patterns predicts that the same time integrals converge to non-zero values of opposite sign (Figure 16, column 2). A combination of latency- and amplitude-based relationships predicts an initial bifurcation of the time integrals of the fast and slow reaction time residuals that then partially re-convergence (Figure 16**,** column 3). We found that our data was most consistent with a mixture of latency- and gain-based effects.

To perform these simulations, we compiled a distribution of reaction times for all correct memory-guided saccades across our subject database. For each simulation we drew 400 random samples from this distribution. To simulate the simple latency-based effect of BOLD signal variability we generated an impulse function, a vector where all but one element is equal to zero, where each element refers to 60ms time bin after the

memory-guided saccade response signal. For each draw from the reaction time distribution we generated an impulse function by inserting a 1 into the vector at the index, which corresponded to the drawn reaction time. We convolved each of the 400 impulse functions with a canonical HRF modeled at the same 60ms resolution. This produced a set of HRF time series whose time of peak amplitude varied with reaction time. We computed the mean HRF time series across all trials as well as the mean HRF time series for fast and slow reaction time trials defined by median split. We simulated residual time series for each trial by subtracting the mean HRF time series from the individual time series and computing the mean of the residual time series for fast and slow reaction time trials. Lastly, we computed the time integral of the mean residual time series for fast and slow trials.

The amplitude-based simulation was performed similarly but with two key differences: 1) for each trial we inserted 1 into all impulse function vectors at the same time index, corresponding to mean reaction time, for all trials. Then we added or subtracted from the 1 a linearly interpolated value between ±0.25 where +0.25 corresponded to the fastest reaction time and -0.25 corresponded to the slowest reaction time. Mixed amplitude and latency based simulations were a hybrid of the two described above. The index of the 1 for each trial's impulse function was selected to coincide with the reaction time on that trial. An additional amplitude modulation factor, as above, was added to the impulse index. To compare the simulated pattern of high temporal resolution residuals to the actual data, we interpolated the brain state residuals time series to a matched temporal resolution using shape preserving piece-wise cubic interpolation (MATLAB).

Mixed amplitude and latency based simulations were a hybrid of the two described above. The index of the 1 for each trial's impulse function was selected to coincide with the reaction time on that trial. An additional amplitude modulation factor, as above, was added to the impulse index. To compare the simulated pattern of high temporal resolution residuals to the actual data, we interpolated the brain state residuals time series to a matched temporal resolution using shape preserving piece-wise cubic interpolation (MATLAB).

## D.8 MEASUREMENTS OF BRAIN STATE VARIABILITY ARE UNAFFECTED BY MOTION

We had observed that total brain state variability decreased with age, and one concern that we had was that this result might not reflect a true developmental change in neural variability, but might instead be a reflection of the more mundane tendency either for children to move more in the scanner than adults, or due to small differences in behavioral performance. If BOLD signal variability resulting from motion-related artifacts or performance were systematically related to brain state variability then our interpretation of the reduction in brain state variability with age might be undermined. We therefore performed a series of control analyses designed to measure and control for these potential relationships.

First, we measured the relationship between total brain state variability and estimated in-scanner motion and found that the two were largely unrelated ($t(334)=1.43$;

p=0.15). Next, we computed the proportion of BOLD signal variability, present within the post-deconvolution residuals, that corresponds to the whole-brain motion templates (see Appendix D.5). This measure, referred to here as motion template variance, which quantifies BOLD signal variability associated with lingering linear effects of motion that were not removed by the deconvolution process, is significantly related to our estimate of in-scanner motion (t(334)=8.58; p=3.71e-16). This indicates that even after rigorous motion controls during the deconvolution step of our fMRI analysis, there are likely still some linear motion artifacts present. We found a small but significant positive relationship between the magnitude of motion template variance and the magnitude of total brain state variability within a session (t(334)=2.1; p=0.037).

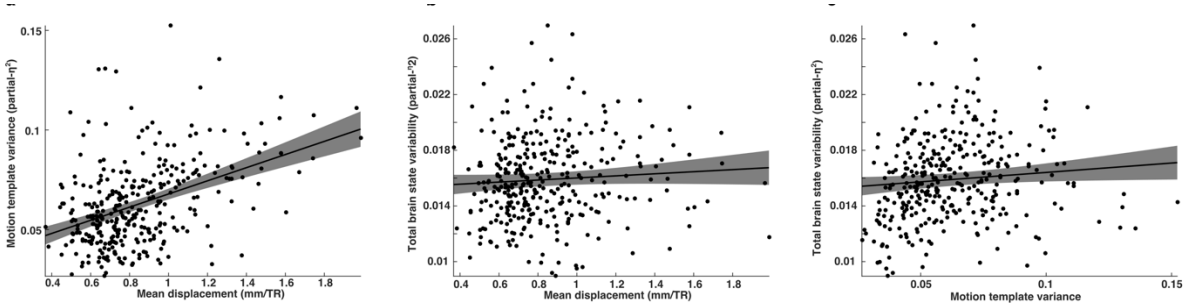


**Figure 17. Brain state variability and motion**

**(a) The proportion of motion and nuisance related variability present in the grey matter residual time series increased with the estimate of average subject per frame displacement. This is variability that was unaccounted for in the session level deconvolution analysis, which included a set of 28 temporally leading and lagging motion regressors. (b) Total brain state variability is uncorrelated with estimates of in-scanner movement. (c) Measurements of brain state variability share a slight positive relationship with measures of residual motion artifacts.**

Although the relationship between brain state variability and movement was small and inconsistent across estimates of in-scanner motion, we sought a more rigorous control. We reasoned that if brain state variability was unrelated to movement-related artifacts, then our finding that brain state variability was reduced in older subjects should still hold if we selectively sub-sampled our data so that we compared a group of adults who moved excessively to a group of children who moved relatively little. To put this idea to the test, we divided our data into two sets, split at the median age of our sample. We based our approach on a mean matching algorithm (see Appendix E) that would selectively draw samples from the two data sets such that, on average, estimated mean in-scanner displacement or motion template variance was identical. Then, we introduced a small bias into the data set that exaggerated the relationship between age and the two motion variables. This caused our mean matching algorithm to over-compensate, resulting in a reversal of the age-motion relationship. We found that, for both in-scanner displacement and motion template variance (data not shown), reversing the relationship between motion and age did not significantly alter our finding that older subjects exhibited less brain state variability than younger subjects (Figure 18).

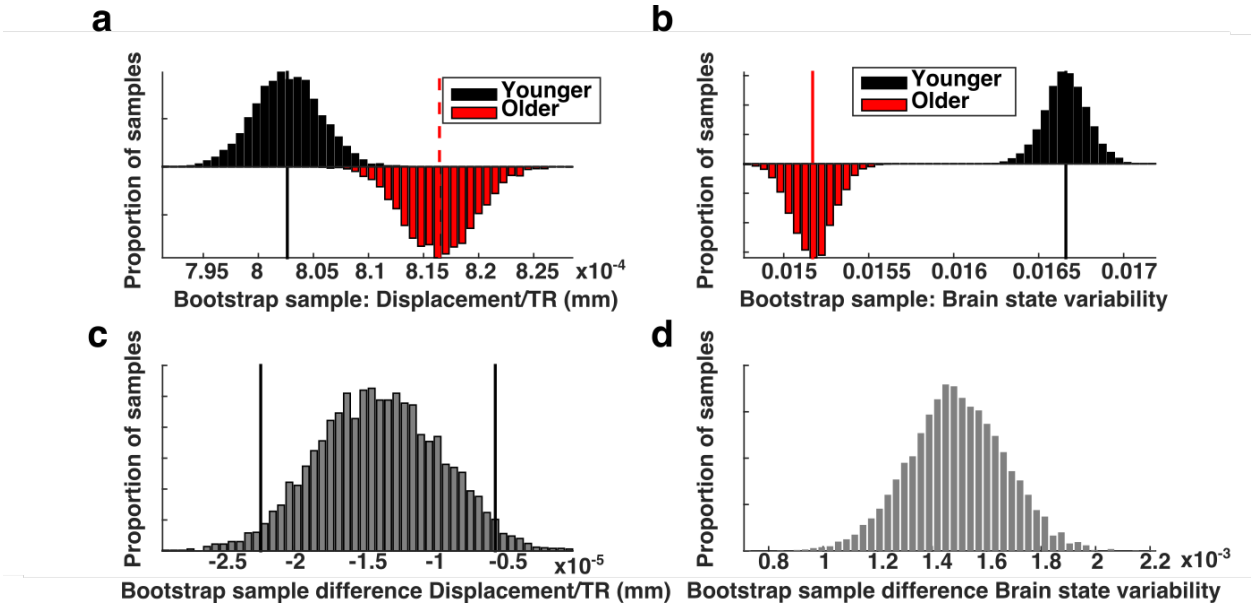


**Figure 18. Brain state variability in high motion adults compared to low motion children**

**a) Biased bootstrap sample distribution of in-scanner motion in which the older subjects (red histogram) moved more than younger subjects (black histogram). b) The corresponding distributions of brain state variability demonstrating that brain state variability is still greater in younger subjects who moved more than adults. Vertical lines in the top two panels represent the means of the distributions. c-d) The bootstrap differences for the corresponding distributions above. Vertical black lines indicate 95% confidence intervals.**

## D.9 DIMENSIONALITY OF BOLD SIGNAL RESIDUALS

For each TR of the BOLD times series residuals, we regressed out the six brain state patterns and the set of motion templates and extracted a vector of voxel values that resided within the brain state mask, producing a high-dimensional time series of doubly

residualized BOLD signal. We estimated the intrinsic dimensionality of these time series using a maximum likelihood estimation procedure [86]. We relied on the implementation of this method provided by Matlab Toolbox for Dimensionality Reduction [93]. We selected this procedure based on two criteria: 1) minimal demands for prespecified parameters, requiring only specification of the “nearest neighbors” parameter, lambda; and 2) the method's rank-order robustness to misspecification of. That is, while misspecifying lambda can alter an estimate of dimensionality, a low dimensional embedding will still tend to be assigned lower estimate of dimensionality than a higher dimensional embedding [86] We computed our dimensionality estimates using lambda = 6..12, for each session and then averaged the resulting dimensionality estimates.

# APPENDIX E

## MEAN MATCHING ALGORITHM

In some of our analyses, we employ a mean matching algorithm to observe how a variable differs between two groups while simultaneously either holding a second confounding variable at a constant value across both groups or reversing its natural relationship across the groups. Our approach to equating the mean value of a confounding variable across groups, which we most often used to match estimates of in-scanner motion between two age groups, is based on an intersection of histograms method. Figure 19 illustrates this. After dividing a dataset into two groups, based on our variable of interest (age, for instance), we construct histograms of the confounding variable (e.g. motion). Comparing the counts within each histogram bin across both data sets and selecting the smaller of the two values determines the intersection of the two histograms. We used a bootstrapping procedure to randomly sample both halves of the data set with replacement, subject to the constraint that, for each sampling iteration, the distributions of the confounding variable from both groups must be equal to the distribution defined by the intersection of their histograms. This constraint guarantees that the mean of the confound variable for both groups for each sampling interaction is

nearly equal (although in practice the, some differences are expected based on the width of the histogram bins). For each matched sample drawn from both groups we also record the mean values of the variable of interest and construct their distributions across all sampling iterations. The difference between distributions of the variable of interest for both groups, after sampling from the matched potions of their histograms, reflects their difference after controlling for the confound variable.

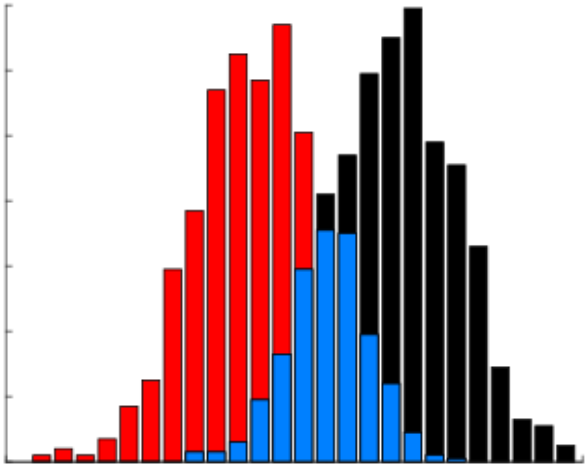

**Figure 19. Mean matching with the intersection of histograms**

**Simulated data illustrating a technique for mean matching based on the intersections of histograms. Red and black histograms represent distributions of variables to be matched on, e.g., in-scanner motion for two groups of subjects from different age groups. By drawing bootstrap samples constrained to for a distribution defined by the intersection (blue) surrogated data sets for the two groups of subjects can be generated in which that matched variable does not differ between them.**

This method of controlling for confound variables can be made even more stringent by biasing the data so that, rather than matching the means of a confound

variable across two groups, it's natural relationship with the groups is reversed. In our analyses, for instance, we wanted to ensure that the decrease in brain state variability across development was not a result of subjects moving less in the scanner as they got older. To do this, we wanted to examine how brain state variability differed between a set of younger subject, who moved relatively little, and older subjects who moved more. If the same brain state variability in the movement-prone adult sample was still less than that observed in the group of younger subjects, then we could be relatively sure that age-related differences in motion artifacts are spuriously driving developmental changes in brain state variability. To appropriately bias the data, we then constructed a secondary dataset in which the relationship between age and the motion variables were amplified. We did this by adding a small linear effect of age to the confounding motion variables. Then we applied the mean matching algorithm described above to this new data set. This procedure effectively amplifies whatever relationship with age is present in the confound variables, causing the mean matching algorithm to over-compensate by selecting sampling data from the set of older subjects that in reality actually moved more than the group of younger subjects.

## BIBLIOGRAPHY


[1] A. D. Baddeley and R. H. Logie, *Working memory: the multiple component model, Miyake A., Shah P., Models of working memory, 1999, 28-61*. Cambridge University Press.

[2] A. Diamond and P. S. Goldman-Rakic, “Comparison of human infants and rhesus monkeys on Piaget's AB task: evidence for dependence on dorsolateral prefrontal cortex.,” *Exp Brain Res*, vol. 74, no. 1, pp. 24–40, 1989.

[3] A. Demetriou, C. Christou, G. Spanoudis, and M. Platsidou, “The Development of mental processing: working memory efficiencey, memory, and thinking,” *Monogr Soc Res Child Dev*, vol. 67, no. 1, pp. i–viii– 1–155– discussion 156, 2002.

[4] T. P. Alloway, S. E. Gathercole, and S. J. Pickering, “Verbal and visuospatial short-term and working memory in children: are they separable?,” *Child Dev*, vol. 77, no. 6, pp. 1698–1716, Nov. 2006.

[5] B. Luna, K. E. Garver, T. A. Urban, N. A. Lazar, and J. A. Sweeney, “Maturation of cognitive processes from late childhood to adulthood.,” *Child Dev*, vol. 75, no. 5, pp. 1357–1372, Sep. 2004.

[6] H. Kwon, A. L. Reiss, and V. Menon, “Neural basis of protracted developmental changes in visuo-spatial working memory.,” *Proc. Natl. Acad. Sci. U.S.A.*, vol. 99, no. 20, pp. 13336–13341, Oct. 2002.

[7] M. E. Thomason, E. Race, B. Burrows, S. Whitfield-Gabrieli, G. H. Glover, and J. D. E. Gabrieli, “Development of Spatial and Verbal Working Memory Capacity in the Human Brain,” *J Cogn Neurosci*, vol. 21, no. 2, pp. 316–332, Feb. 2009.

[8] E. A. Crone, C. Wendelken, S. Donohue, L. van Leijenhorst, and S. A. Bunge, “Neurocognitive development of the ability to manipulate information in working memory,” *Proc. Natl. Acad. Sci. U.S.A.*, vol. 103, no. 24, pp. 9315–9320, Jun. 2006.

[9] D. P. Munoz, I. T. Armstrong, K. A. Hampton, and K. D. Moore, “Altered Control of Visual Fixation and Saccadic Eye Movements in Attention-Deficit Hyperactivity Disorder,” *Journal of Neurophysiology*, vol. 90, no. 1, pp. 503–514, Jul. 2003.

[10] S. Kaiser, A. Roth, M. Rentrop, H.-C. Friederich, S. Bender, and M. Weisbrod, “Intra-individual reaction time variability in schizophrenia, depression and borderline personality disorder,” *Brain Cogn*, vol. 66, no. 1, pp. 73–82, Feb. 2008.

[11] S. MacDonald, L. Nyberg, and L. Bäckman, “Intra-individual variability in behavior: links to brain structure, neurotransmission and neuronal activity,” *Trends in Neurosciences*, vol. 29, no. 8, pp. 474–480, 2006.
[12] A. M. Fjell, L. T. Westlye, I. K. Amlien, and K. B. Walhovd, “Reduced white matter integrity is related to cognitive instability.,” *J. Neurosci.*, vol. 31, no. 49, pp. 18060–18072, Dec. 2011.
[13] C. K. Tamnes, A. M. Fjell, L. T. Westlye, Y. Østby, and K. B. Walhovd, “Becoming consistent: developmental reductions in intraindividual variability in reaction time are related to white matter integrity.,” *J. Neurosci.*, vol. 32, no. 3, pp. 972–982, Jan. 2012.
[14] A. R. McIntosh, N. Kovacevic, and R. J. Itier, “Increased brain signal variability accompanies lower behavioral variability in development.,” *PLoS Comput. Biol.*, vol. 4, no. 7, p. e1000106, 2008.
[15] B. Misic, T. Mills, M. J. Taylor, and A. R. McIntosh, “Brain Noise Is Task Dependent and Region Specific,” *Journal of Neurophysiology*, vol. 104, no. 5, pp. 2667–2676, Nov. 2010.
[16] D. D. Garrett, N. Kovacevic, A. R. McIntosh, and C. L. Grady, “Blood Oxygen Level-Dependent Signal Variability Is More than Just Noise,” *J. Neurosci.*, vol. 30, no. 14, pp. 4914–4921, Apr. 2010.
[17] S. Marek, K. Hwang, W. Foran, M. N. Hallquist, and B. Luna, “The Contribution of Network Organization and Integration to the Development of Cognitive Control,” *PLoS Biol*, vol. 13, no. 12, pp. e1002328–25, Dec. 2015.
[18] O. Hikosaka and R. H. Wurtz, “Visual and oculomotor functions of monkey substantia nigra pars reticulata. III. Memory-contingent visual and saccade responses.,” *Journal of Neurophysiology*, vol. 49, no. 5, pp. 1268–1284, May 1983.
[19] M. V. Chafee and P. S. Goldman-Rakic, “Matching patterns of activity in primate prefrontal area 8a and parietal area 7ip neurons during a spatial working memory task.,” *Journal of Neurophysiology*, vol. 79, no. 6, pp. 2919–2940, Jun. 1998.
[20] R. Levy and P. S. Goldman-Rakic, “Segregation of working memory functions within the dorsolateral prefrontal cortex,” *Exp Brain Res*, vol. 133, no. 1, pp. 23–32, May 2000.
[21] M. D'Esposito and B. R. Postle, “The Cognitive Neuroscience of Working Memory,” *Annu. Rev. Psychol.*, vol. 66, no. 1, pp. 115–142, Jan. 2015.
[22] M. A. Sommer and R. H. Wurtz, “Frontal eye field sends delay activity related to movement, memory, and vision to the superior colliculus.,” *Journal of Neurophysiology*, vol. 85, no. 4, pp. 1673–1685, Apr. 2001.
[23] C. L. Colby, J. R. Duhamel, and M. E. Goldberg, “Visual, presaccadic, and cognitive activation of single neurons in monkey lateral intraparietal area.,” *Journal of Neurophysiology*, vol. 76, no. 5, pp. 2841–2852, Nov. 1996.
[24] M. M. Umeno and M. E. Goldberg, “Spatial processing in the monkey frontal eye field. I. Predictive visual responses.,” *Journal of Neurophysiology*, vol. 78, no. 3, pp. 1373–1383, Sep. 1997.
[25] M. R. G. Brown, J. F. X. DeSouza, H. C. Goltz, K. Ford, R. S. Menon, M. A.

Goodale, and S. Everling, “Comparison of memory- and visually guided saccades using event-related fMRI.,” *Journal of Neurophysiology*, vol. 91, no. 2, pp. 873–889, Feb. 2004.

[26] J. T. Serences, E. F. Ester, E. K. Vogel, and E. Awh, “Stimulus-specific delay activity in human primary visual cortex.,” *Psychological Science*, vol. 20, no. 2, pp. 207–214, Feb. 2009.

[27] S. A. Harrison and F. Tong, “Decoding reveals the contents of visual working memory in early visual areas.,” *Nature*, vol. 458, no. 7238, pp. 632–635, Apr. 2009.

[28] J. Fukushima, T. Hatta, and K. Fukushima, “Development of voluntary control of saccadic eye movements. I. Age-related changes in normal children.,” *Brain Dev.*, vol. 22, no. 3, pp. 173–180, May 2000.

[29] E. L. Irving, M. J. Steinbach, L. Lillakas, R. J. Babu, and N. Hutchings, “Horizontal Saccade Dynamics across the Human Life Span,” *Invest. Ophthalmol. Vis. Sci.*, vol. 47, no. 6, pp. 2478–7, Jun. 2006.

[30] D. P. Munoz, J. R. Broughton, J. E. Goldring, and I. T. Armstrong, “Age-related performance of human subjects on saccadic eye movement tasks.,” *Exp Brain Res*, vol. 121, no. 4, pp. 391–400, Aug. 1998.

[31] P. M. Fitts and J. R. Peterson, “Information capacity of discrete motor responses.,” *Journal of Experimental Psychology*, vol. 67, no. 2, pp. 103–112, 1964.

[32] T. Paus, V. Babenko, and T. Radil, “Development of an ability to maintain verbally instructed central gaze fixation studied in 8-to 10-year-old children,” *International journal of Psychophysiology*, 1990.

[33] J. I. Gold and M. N. Shadlen, “Neural computations that underlie decisions about sensory stimuli,” pp. 1–7, Dec. 2000.

[34] C.-C. Wu, O.-S. Kwon, and E. Kowler, “Fitts’s Law and speed/accuracy trade-offs during sequences of saccades: Implications for strategies of saccadic planning,” *Vision Res.*, vol. 50, no. 21, pp. 2142–2157, Oct. 2010.

[35] C. M. Harris and D. M. Wolpert, “The Main Sequence of Saccades Optimizes Speed-accuracy Trade-off,” *Biol Cybern*, vol. 95, no. 1, pp. 21–29, Mar. 2006.

[36] B. A. Purcell, J. D. Schall, G. D. Logan, and T. J. Palmeri, “From salience to saccades: multiple-alternative gated stochastic accumulator model of visual search.,” *J. Neurosci.*, vol. 32, no. 10, pp. 3433–3446, Mar. 2012.

[37] J. Palmer, A. C. Huk, and M. N. Shadlen, “The effect of stimulus strength on the speed and accuracy of a perceptual decision.,” *J Vis*, vol. 5, no. 5, pp. 376–404, May 2005.

[38] J. I. Gold and M. N. Shadlen, “The Neural Basis of Decision Making,” *Annu. Rev. Neurosci.*, vol. 30, no. 1, pp. 535–574, Jul. 2007.

[39] R. Ratcliff and J. N. Rouder, “Modeling Response Times for Two-Choice Decisions,” *Psychological Science*, vol. 9, no. 5, pp. 347–356, Sep. 1998.

[40] T. Paus, A. Zijdenbos, K. Worsley, D. L. Collins, J. Blumenthal, J. N. Giedd, J. L. Rapoport, and A. C. Evans, “Structural Maturation of Neural Pathways in Children and Adolescents: In Vivo Study,” *Science*, vol. 283, no. 5409, pp. 1908–1911, Mar. 1999.

[41] P. W. Glimcher and D. L. Sparks, “Movement selection in advance of action in the superior colliculus.,” *Nature*, vol. 355, no. 6360, pp. 542–545, Feb. 1992.
[42] O. Hikosaka and R. H. Wurtz, “Modification of saccadic eye movements by GABA-related substances. II. Effects of muscimol in monkey substantia nigra pars reticulata,” *Journal of Neurophysiology*, vol. 53, no. 1, pp. 292–308, Jan. 1985.
[43] C.-C. Lo and X.-J. Wang, “Cortico–basal ganglia circuit mechanism for a decision threshold in reaction time tasks,” *Nat Neurosci*, vol. 9, no. 7, pp. 956–963, Jun. 2006.
[44] G. Aston-Jones and J. D. Cohen, “An integrative theory of locus coeruleus-norepinephrine function: adaptive gain and optimal performance,” *Annu. Rev. Neurosci.*, vol. 28, no. 1, pp. 403–450, 2005.
[45] P. Bentley, M. Husain, and R. J. Dolan, “Effects of cholinergic enhancement on visual stimulation, spatial attention, and spatial working memory.,” *Neuron*, vol. 41, no. 6, pp. 969–982, Mar. 2004.
[46] B. Noudoost and T. Moore, “Control of visual cortical signals by prefrontal dopamine,” *Nature*, 2011.
[47] F. S. Chance, L. F. Abbott, and A. D. Reyes, “Gain modulation from background synaptic input.,” *Neuron*, vol. 35, no. 4, pp. 773–782, Aug. 2002.
[48] K. H. Britten, W. T. Newsome, M. N. Shadlen, S. Celebrini, and J. A. Movshon, “A relationship between behavioral choice and the visual responses of neurons in macaque MT,” *Visual Neuroscience*, vol. 13, no. 1, pp. 87–100, 1996.
[49] M. R. Cohen and J. H. R. Maunsell, “A neuronal population measure of attention predicts behavioral performance on individual trials.,” *J. Neurosci.*, vol. 30, no. 45, pp. 15241–15253, Nov. 2010.
[50] A. D. Wagner, D. L. Schacter, M. Rotte, W. Koutstaal, A. Maril, A. M. Dale, B. R. Rosen, and R. L. Buckner, “Building memories: remembering and forgetting of verbal experiences as predicted by brain activity.,” *Science*, vol. 281, no. 5380, pp. 1188–1191, Aug. 1998.
[51] D. J. Heeger and D. Ress, “Neuronal correlates of perception in early visual cortex,” *Nat Neurosci*, vol. 6, no. 4, pp. 414–421, Apr. 2003.
[52] M. N. Shadlen, K. H. Britten, W. T. Newsome, and J. A. Movshon, “A computational analysis of the relationship between neuronal and behavioral responses to visual motion.,” *J. Neurosci.*, vol. 16, no. 4, pp. 1486–1510, Feb. 1996.
[53] M. R. Cohen and A. Kohn, “Measuring and interpreting neuronal correlations,” *Nature Neuroscience*, vol. 14, no. 7, pp. 811–819, Jul. 2011.
[54] J. Gonzalez-Castillo, Z. S. Saad, D. A. Handwerker, S. J. Inati, N. Brenowitz, and P. A. Bandettini, “Whole-brain, time-locked activation with simple tasks revealed using massive averaging and model-free analysis,” *Proc. Natl. Acad. Sci. U.S.A.*, vol. 109, no. 14, pp. 5487–5492, Apr. 2012.
[55] M. E. Raichle, A. M. MacLeod, A. Z. Snyder, W. J. Powers, D. A. Gusnard, and G. L. Shulman, “A default mode of brain function.,” *Proc. Natl. Acad. Sci. U.S.A.*, vol. 98, no. 2, pp. 676–682, Jan. 2001.
[56] M. D. Fox, A. Z. Snyder, J. M. Zacks, and M. E. Raichle, “Coherent spontaneous

activity accounts for trial-to-trial variability in human evoked brain responses.," *Nat Neurosci*, vol. 9, no. 1, pp. 23–25, Jan. 2006.
[57] H. Nienborg and B. G. Cumming, "Decision-related activity in sensory neurons reflects more than a neuron's causal effect.," *Nature*, vol. 459, no. 7243, pp. 89–92, May 2009.
[58] E. Eldar, J. D. Cohen, and Y. Niv, "The effects of neural gain on attention and learning," *Nat Neurosci*, vol. 16, no. 8, pp. 1146–1153, Aug. 2013.
[59] C. J. McAdams and J. H. Maunsell, "Effects of attention on orientation-tuning functions of single neurons in macaque cortical area V4.," *J. Neurosci.*, vol. 19, no. 1, pp. 431–441, Jan. 1999.
[60] S. Treue and J. C. Martínez Trujillo, "Feature-based attention influences motion processing gain in macaque visual cortex.," *Nature*, vol. 399, no. 6736, pp. 575–579, Jun. 1999.
[61] N. C. Rabinowitz, R. L. Goris, M. Cohen, and E. P. Simoncelli, "Attention stabilizes the shared gain of V4 populations," *Elife*, 2015.
[62] D. A. Handwerker, J. M. Ollinger, and M. D'Esposito, "Variation of BOLD hemodynamic responses across subjects and brain regions and their effects on statistical analyses," *NeuroImage*, vol. 21, no. 4, pp. 1639–1651, Apr. 2004.
[63] M. L. Furey, P. Pietrini, and J. V. Haxby, "Cholinergic enhancement and increased selectivity of perceptual processing during working memory.," *Science*, vol. 290, no. 5500, pp. 2315–2319, Dec. 2000.
[64] M. Sarter and J. P. Bruno, "Cognitive functions of cortical acetylcholine: toward a unifying hypothesis.," *Brain Res. Brain Res. Rev.*, vol. 23, no. 1, pp. 28–46, Feb. 1997.
[65] D. Standage, H. You, D.-H. Wang, and M. C. Dorris, "Gain Modulation by an Urgency Signal Controls the Speed–Accuracy Trade-Off in a Network Model of a Cortical Decision Circuit," *Front. Comput. Neurosci.*, vol. 5, pp. 1–14, 2011.
[66] R. P. Heitz and J. D. Schall, "Neural mechanisms of speed-accuracy tradeoff.," *Neuron*, vol. 76, no. 3, pp. 616–628, Nov. 2012.
[67] S. Ferraina, M. Paré, and R. H. Wurtz, "Comparison of cortico-cortical and cortico-collicular signals for the generation of saccadic eye movements.," *Journal of Neurophysiology*, vol. 87, no. 2, pp. 845–858, Feb. 2002.
[68] M. E. Larkum, W. Senn, and H.-R. Lüscher, "Top-down dendritic input increases the gain of layer 5 pyramidal neurons.," *Cereb. Cortex*, vol. 14, no. 10, pp. 1059–1070, Oct. 2004.
[69] T. Moore and K. M. Armstrong, "Selective gating of visual signals by microstimulation of frontal cortex.," *Nature*, vol. 421, no. 6921, pp. 370–373, Jan. 2003.
[70] D. J. Chandler, W. J. Gao, and B. D. Waterhouse, "Heterogeneous organization of the locus coeruleus projections to prefrontal and motor cortices," *Proc. Natl. Acad. Sci. U.S.A.*, vol. 111, no. 18, pp. 6816–6821, May 2014.
[71] M. Luciana, P. F. Collins, and R. A. Depue, "Opposing roles for dopamine and serotonin in the modulation of human spatial working memory functions.," *Cereb. Cortex*, vol. 8, no. 3, pp. 218–226, Apr. 1998.
[72] A. Rokem, A. N. Landau, D. Garg, W. Prinzmetal, and M. A. Silver, "Cholinergic

enhancement increases the effects of voluntary attention but does not affect involuntary attention.," *Neuropsychopharmacology*, vol. 35, no. 13, pp. 2538–2544, Dec. 2010.
[73] K.-J. Bär, F. de la Cruz, A. Schumann, S. Koehler, H. Sauer, H. Critchley, and G. Wagner, "Functional connectivity and network analysis of midbrain and brainstem nuclei.," *NeuroImage*, vol. 134, pp. 53–63, Apr. 2016.
[74] D. J. Simmonds, M. N. Hallquist, M. Asato, and B. Luna, "Developmental stages and sex differences of white matter and behavioral development through adolescence: a longitudinal diffusion tensor imaging (DTI) study," *NeuroImage*, vol. 92, pp. 356–368, 2014.
[75] E. L. Dennis, N. Jahanshad, K. L. McMahon, G. I. de Zubicaray, N. G. Martin, I. B. Hickie, A. W. Toga, M. J. Wright, and P. M. Thompson, "Development of brain structural connectivity between ages 12 and 30: a 4-Tesla diffusion imaging study in 439 adolescents and adults.," *NeuroImage*, vol. 64, pp. 671–684, Jan. 2013.
[76] H. Nienborg and B. Cumming, "Correlations between the activity of sensory neurons and behavior: how much do they tell us about a neuron's causality?," *Current Opinion in Neurobiology*, vol. 20, no. 3, pp. 376–381, Jun. 2010.
[77] S. Lippe, "Differential maturation of brain signal complexity in the human auditory and visual system," *Front. Hum. Neurosci.*, vol. 3, pp. 1–9, 2009.
[78] D. D. Garrett, N. Kovacevic, A. R. McIntosh, and C. L. Grady, "The Importance of Being Variable," *J. Neurosci.*, vol. 31, no. 12, pp. 4496–4503, Mar. 2011.
[79] C. Y. Liu, A. P. Krishnan, L. Yan, R. X. Smith, E. Kilroy, J. R. Alger, J. M. Ringman, and D. J. J. Wang, "Complexity and synchronicity of resting state blood oxygenation level-dependent (BOLD) functional MRI in normal aging and cognitive decline," *J. Magn. Reson. Imaging*, vol. 38, no. 1, pp. 36–45, Dec. 2012.
[80] A. C. Yang, C. C. Huang, H. L. Yeh, M. E. Liu, C. J. Hong, P. C. Tu, J. F. Chen, N. E. Huang, C. K. Peng, C. P. Lin, and S. J. Tsai, "Complexity of spontaneous BOLD activity in default mode network is correlated with cognitive function in normal male elderly: a multiscale entropy analysis," *NBA*, pp. 1–11, Jun. 2012.
[81] D. D. Garrett, A. R. McIntosh, and C. L. Grady, "Brain Signal Variability is Parametrically Modifiable.," *Cereb. Cortex*, vol. 24, no. 11, pp. 2931–2940, Nov. 2014.
[82] A. Ghosh, Y. Rho, A. R. McIntosh, R. Kötter, and V. K. Jirsa, "Noise during Rest Enables the Exploration of the Brain's Dynamic Repertoire," *PLoS Comput. Biol.*, vol. 4, no. 10, pp. e1000196–12, Oct. 2008.
[83] B. Luna, S. Marek, B. Larsen, B. Tervo-Clemmens, and R. Chahal, "An Integrative Model of the Maturation of Cognitive Control," *Annu. Rev. Neurosci.*, vol. 38, no. 1, pp. 151–170, Jul. 2015.
[84] G. Tononi, O. Sporns, and G. M. Edelman, "A measure for brain complexity: relating functional segregation and integration in the nervous system," *Proc. Natl. Acad. Sci. U.S.A.*, vol. 91, no. 11, pp. 5033–5037, May 1994.
[85] K. J. Friston, C. D. Frith, P. F. Liddle, and R. S. Frackowiak, "Functional connectivity: the principal-component analysis of large (PET) data sets.," *J.*

*Cereb. Blood Flow Metab.*, vol. 13, no. 1, pp. 5–14, Jan. 1993.
[86] E. Levina and P. J. Bickel, “Maximum likelihood estimation of intrinsic dimension,” *Advances in neural information …*, 2004.
[87] C. L. Grady and D. D. Garrett, “Understanding variability in the BOLD signal and why it matters for aging.,” *Brain Imaging Behav*, vol. 8, no. 2, pp. 274–283, Jun. 2014.
[88] P. I. Yakovlev and A. Lecours, “The myelogenetic cycles of regional maturation of the brain,” in *Regional Development of the Brain in Early Life*, A. Minkowski, Ed. Blackwell, 1967, pp. 3–70.
[89] N. Gogtay, J. N. Giedd, L. Lusk, K. M. Hayashi, D. Greenstein, A. C. Vaituzis, T. F. Nugent III, D. H. Herman, L. S. Clasen, A. W. Toga, J. L. Rapoport, and P. M. Thompson, “Dynamic mapping of human cortical development during childhood through early adulthood,” *Proc. Natl. Acad. Sci. U.S.A.*, vol. 101, no. 21, pp. 8174–8179, May 2004.
[90] T. D. Frank, A. Daffertshofer, P. J. Beek, and H. Haken, “Impacts of noise on a field theoretical model of the human brain,” *Physica D: Nonlinear …*, vol. 127, no. 3, pp. 233–249, 1999.
[91] S.-C. Li, T. von Oertzen, and U. Lindenberger, “A neurocomputational model of stochastic resonance and aging,” *Neurocomputing*, vol. 69, no. 13, pp. 1553–1560, Aug. 2006.
[92] M. R. Cohen, M. R. Cohen, J. H. R. Maunsell, and J. H. R. Maunsell, “Attention improves performance primarily by reducing interneuronal correlations,” *Nature Neuroscience*, vol. 12, no. 12, pp. 1594–1600, Dec. 2009.
[93] L. Van der Maaten and E. O. Postma, “Matlab toolbox for dimensionality reduction,” *MICC*, 2007.